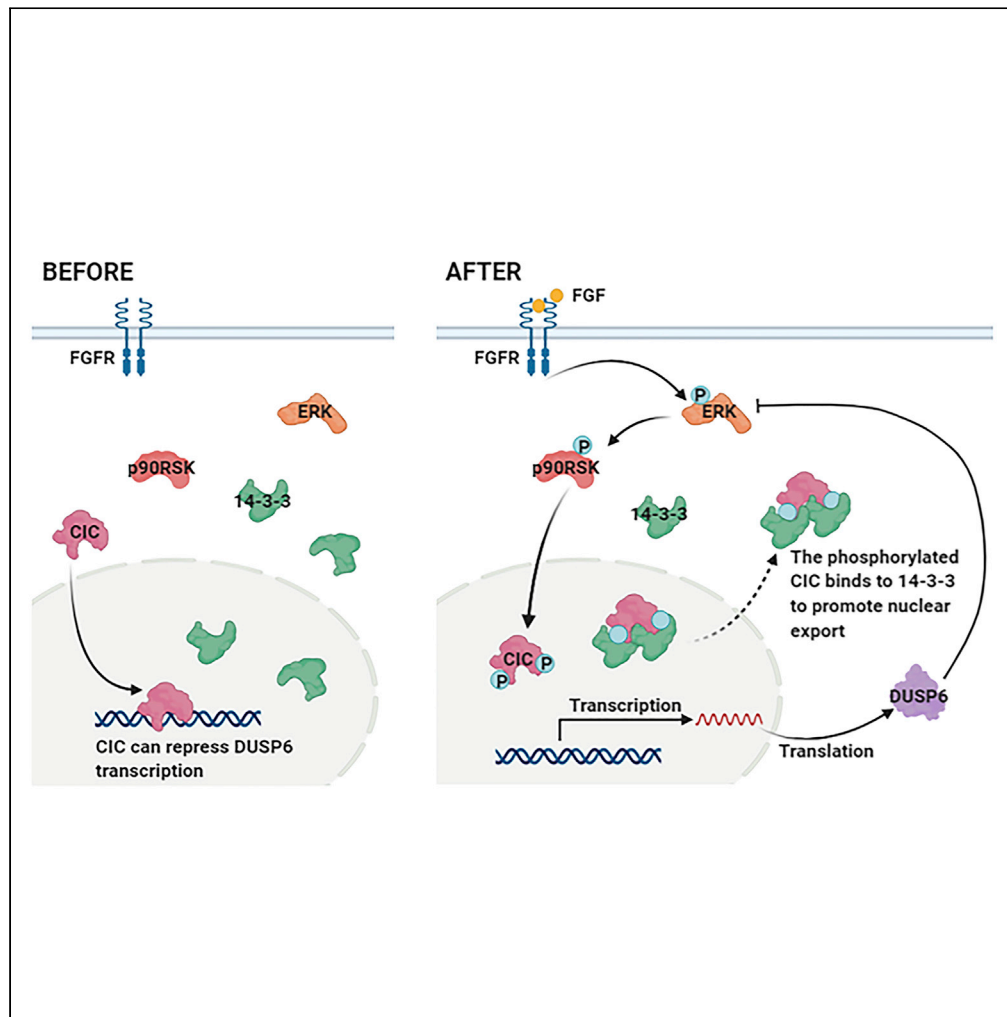


Article

# CIC Is a Mediator of the ERK1/2-DUSP6 Negative Feedback Loop



Yibo Ren, Zhenlin Ouyang, Zhanwu Hou, ..., Huadong Liu, Yurong Wen, Yongping Shao

yurong.wen@xjtu.edu.cn (Y.W.)  
yongping.shao@mail.xjtu.edu.cn (Y.S.)

**HIGHLIGHTS**

CIC represses DUSP6 transcription through direct promoter binding

p90RSK phosphorylates CIC at S173 and S301 sites

S173/S301 phosphorylated CIC binds to 14-3-3 to promote its nuclear export

ERK/p90RSK signaling regulates the subcellular localization of CIC-DUX4 protein

Ren et al., iScience 23, 101635  
November 20, 2020 © 2020  
The Authors.  
<https://doi.org/10.1016/j.isci.2020.101635>



## Article

## CIC Is a Mediator of the ERK1/2-DUSP6 Negative Feedback Loop

Yibo Ren,<sup>1</sup> Zhenlin Ouyang,<sup>2</sup> Zhanwu Hou,<sup>3</sup> Yuwei Yan,<sup>3</sup> Zhe Zhi,<sup>1</sup> Mengjin Shi,<sup>3</sup> Mengtao Du,<sup>3</sup> Huadong Liu,<sup>3</sup> Yurong Wen,<sup>2,\*</sup> and Yongping Shao<sup>1,4,5,\*</sup>

## SUMMARY

**DUSP6 functions as an important negative feedback component of the MAPK/ERK signaling pathway. Although DUSP6 expression is tightly regulated by ERK1/2 signaling, the molecular mechanism of this regulation remains partially understood. In this work, we show that the transcriptional repressor CIC functions downstream of the ERK1/2 signaling to negatively regulate DUSP6 expression. CIC directly represses DUSP6 transcription by binding to three cis-regulatory elements (CREs) in DUSP6 promoter. p90RSK, a downstream target of ERK1/2, phosphorylates CIC at S173 and S301 sites, which creates a 14-3-3 recognition motif, resulting in 14-3-3-mediated nuclear export of CIC and derepression of DUSP6. Finally, we demonstrate that the oncogenic CIC-DUX4 fusion protein acts as a transcriptional activator of DUSP6 and its nuclear/cytoplasmic distribution remains regulated by ERK1/2 signaling. These results complete an ERK1/2/p90RSK/CIC/DUSP6 negative feedback circuit and elucidate the molecular mechanism of how RTK/MAPK signaling harnesses the transcriptional repressor activity of CIC in mammalian cells.**

## INTRODUCTION

The extracellular signal-regulated kinase 1/2 (ERK1/2) mitogen-activated protein kinase (MAPK) signaling pathway regulates a large array of cellular activities including proliferation, apoptosis, differentiation, and transformation (Chang and Karin, 2001; Johnson and Lapadat, 2002; Pearson et al., 2001). Aberrant activation of this pathway leads to deregulated proliferation and malignant transformation in model organisms and is associated with many human cancers (Dhillon et al., 2007). As a result, the ERK1/2 MAPK pathway is under the tight control of multiple negative regulators that act on almost every component of the pathway. Interestingly, many of these negative regulators themselves are targets of the ERK1/2 MAPK pathway so that negative feedback loops are established to maintain cellular homeostasis (Lake et al., 2016).

Dual-specificity phosphatase 6 (DUSP6) is a member of the DUSP family phosphatases responsible for dephosphorylation and inactivation of the MAPKs (Huang and Tan, 2012). As an important player of the negative feedback network of the ERK1/2 signaling pathway, DUSP6 is one of the immediate-early genes induced by mitogen stimulation and conversely inactivates ERK1/2 by dephosphorylating the pThr/pTyr residues in the activation loop of ERK1/2 (Zeliadt et al., 2008). DUSP6 expression correlates very tightly with the ERK1/2 pathway activity. For example, FGF treatment in NIH3T3 cells rapidly induces the transcription of DUSP6 (Ekerot et al., 2008), whereas blocking constitutive ERK1/2 signaling in melanoma cells leads to immediate shutdown of DUSP6 transcription (Packer et al., 2009; Pratilas et al., 2009).

The molecular mechanism of how DUSP6 is regulated by ERK1/2 signaling is only partially understood. Studies have shown that induction of DUSP6 by FGF is mediated by direct binding of the ERK1/2-responsive transcription factor ETS1 to DUSP6 promoter (Ekerot et al., 2008; Zhang et al., 2010). Although the ERK1/2-ETS1-DUSP6 axis nicely explains the rapid induction of DUSP6 by mitogen stimulation, the question of how DUSP6 transcription is timely turned off (within a couple hours) upon ERK1/2 signaling blockade remains unanswered.

CIC is a transcriptional repressor originally identified in *Drosophila* where it acts in a default repression mechanism downstream of the receptor tyrosine kinase (RTK) signaling to regulate the cell growth and

<sup>1</sup>Frontier Institute of Science and Technology, Xi'an Jiaotong University, Xi'an, 710049, China

<sup>2</sup>Talent Highland, The First Affiliated Hospital, Xi'an Jiaotong University, Xi'an, 710061, China

<sup>3</sup>Key Laboratory of Biomedical Information Engineering of Ministry of Education, School of Life Science and Technology, Xi'an Jiaotong University, Xi'an 710049, China

<sup>4</sup>Department of Dermatology, The Second Affiliated Hospital, Xi'an Jiaotong University, Xi'an 710049, China

<sup>5</sup>Lead Contact

\*Correspondence: yurong.wen@xjtu.edu.cn (Y.W.), yongping.shao@mail.xjtu.edu.cn (Y.S.)

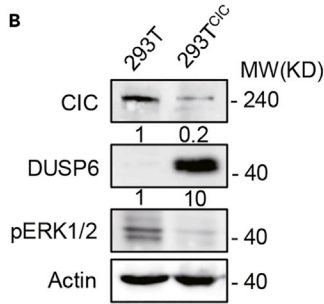
<https://doi.org/10.1016/j.isci.2020.101635>



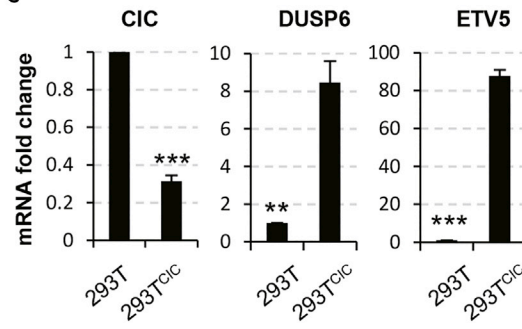
A



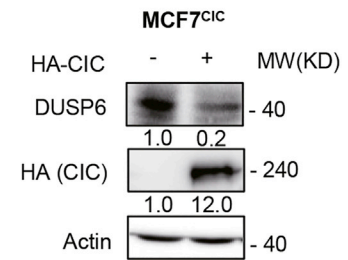
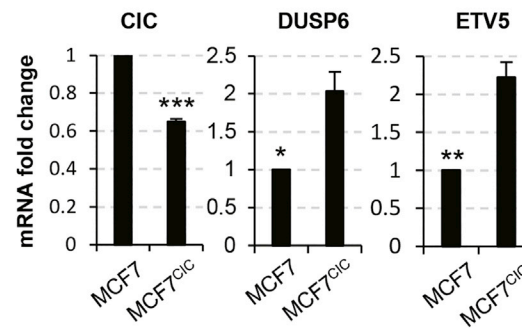
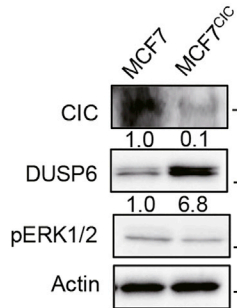
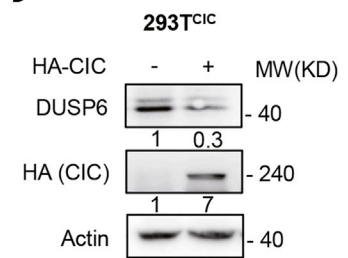
B



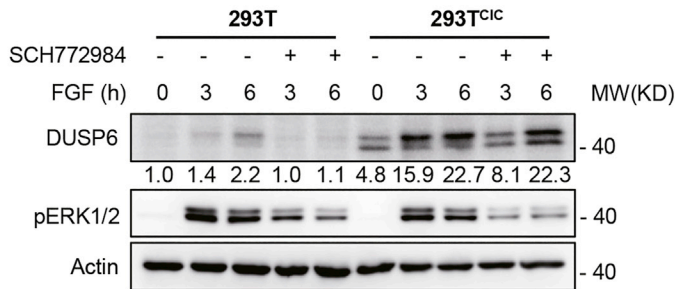
C



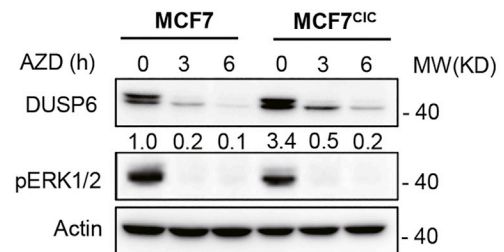
D



E



F



G

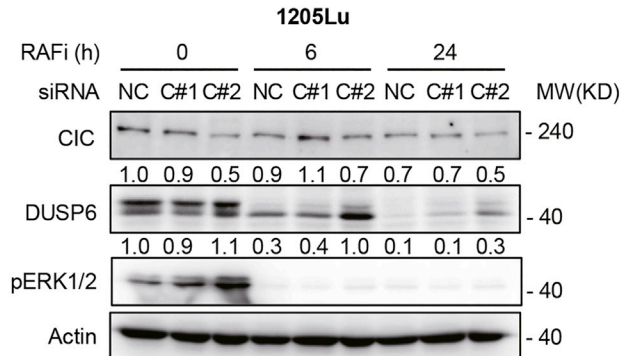


**Figure 1. CIC Functions Downstream of ERK1/2 Signaling to Repress DUSP6 Transcription**

(A) Sequencing verification of CIC knockout in 293T<sup>CIC</sup> and MCF7<sup>CIC</sup> cells.

(B) Western blot analysis of lysates from 293T/293T<sup>CIC</sup> cells (top) or from MCF7/MCF7<sup>CIC</sup> cells (bottom).

(C) q-RT PCR analysis of CIC, DUSP6, and ETV5 transcriptional expression in 293T/293T<sup>CIC</sup> cells (top) or in MCF7/MCF7<sup>CIC</sup> cells (bottom). Data are represented as mean  $\pm$  SEM (N = 3). Significance was determined by student two-tailed t test, \*p < 0.05; \*\*p < 0.01; \*\*\*p < 0.001.

(D) 293T<sup>CIC</sup> (top) or MCF7<sup>CIC</sup> (bottom) cells were transfected with or without HA-CIC expressing plasmid for 48 h before lysis for western blot analysis.

(E) 293T and 293T<sup>CIC</sup> cells were treated with 10 ng/mL FGF for various times in the presence or absence of the ERK inhibitor, SCH772984 (10  $\mu$ M), and lysed for western blot analysis.

(F) MCF7 and MCF7<sup>CIC</sup> cells were treated with 10  $\mu$ M MEK inhibitor AZD6244 for 0, 3, 6 h and lysed for western blot analysis. AZD6244 was used because the ERK inhibitor SCH772984 was not effective to block the ERK signaling in MCF7 cells.

(G) 1205Lu cells were transfected with non-targeting control or CIC-specific siRNAs for 72 h and then treated with 2  $\mu$ M RAF inhibitor, PLX4032, for 0, 6, 24 h. Cells were lysed for western blot analysis.

See also [Figure S1](#).

development of *Drosophila* (Ajuria et al., 2011; Jimenez et al., 2000; Lim et al., 2013; Tseng et al., 2007). CIC-mediated repression of RTK/MAPK pathway genes requires the presence of the Groucho co-repressor in *Drosophila* (Ajuria et al., 2011; Fores et al., 2015; Jennings and Ish-Horowitz, 2008; Jimenez et al., 2000) or of the SIN3 histone deacetylating complex in mammalian cells (Weissmann et al., 2018). Conversely, the RTK/MAPK signaling has been shown to negate CIC's repressor activity through regulating its degradation and/or subcellular distribution in *Drosophila* (Ajuria et al., 2011; Astigarraga et al., 2007; Jimenez et al., 2000; Roch et al., 2002; Tseng et al., 2007). In melanoma cells, CIC can be phosphorylated by MAPK-activated protein kinase-1 (p90RSK) at Ser173 within the HMG domain, which promotes its interaction with 14-3-3 and consequentially blocks its DNA binding (Dissanayake et al., 2011). Previous transcriptome profiling studies in CIC-depleted cells have scored multiple negative regulators of the RTK/MAPK pathway such as *SPRY* and *DUSP* family genes as potential targets of CIC (LeBlanc et al., 2017; Wang et al., 2017; Weissmann et al., 2018), but the detailed regulation mechanisms are still unknown.

In this study, we show that CIC directly represses the transcription of *DUSP6* through binding to several *cis*-regulatory elements (CREs) in *DUSP6* promoter. In addition, we identified an ERK1/2/p90RSK signaling axis that controls the nuclear/cytoplasmic distribution of CIC. Mitogen responsive p90RSK phosphorylates CIC at two sites (S173 and S301), which creates a 14-3-3 recognition motif and results in nuclear export of CIC through 14-3-3 binding, ultimately leading to derepression of CIC target genes. These results complete an ERK1/2/p90RSK/CIC/*DUSP6* negative feedback circuit and elucidate the molecular mechanism of how RTK/MAPK signaling harnesses the transcriptional repressor activity of CIC in mammalian cells.

## RESULTS

### CIC Is a Transcription Repressor of *DUSP6* Downstream of ERK Signaling

Although CIC has been shown to repress some MAPK pathway genes (Gleize et al., 2015; LeBlanc et al., 2017; Weissmann et al., 2018), whether it regulates *DUSP6*, an important negative regulator of the ERK signaling remains unknown. Using CRISPR-Cas9 technique, we generated two CIC-knockout cell lines, 293T<sup>CIC</sup> and MCF7<sup>CIC</sup>, to investigate the impact of CIC depletion on *DUSP6* expression. Targeted disruption of CIC exon in the two cell lines was verified by DNA sequencing (Figure 1A). The 293T<sup>CIC</sup> cells have one base insertion before the CIC-HMG domain, causing a frameshift mutation and truncation of CIC protein. The MCF7<sup>CIC</sup> cells have a deletion of four amino acids upstream the CIC-HMG domain, which results in CIC protein degradation (Figure S1). Both 293T<sup>CIC</sup> and MCF7<sup>CIC</sup> cells had much reduced CIC protein levels when compared with the parental cells, which correlated with increased expressions of *DUSP6* and *ETV5* (a known CIC target gene), and decreased levels of phospho-ERK1/2, a substrate of *DUSP6* (Figures 1B and 1C). Overexpression of CIC in 293T<sup>CIC</sup> or MCF7<sup>CIC</sup> cells, however, reduced *DUSP6* expression (Figure 1D). These results suggested that CIC functions as a transcription repressor of *DUSP6*.

Since ERK signaling controls the transcription expression of *DUSP6* and CIC was deemed to be a downstream effector of the ERK signaling, we wondered whether CIC mediates the regulation of *DUSP6* by ERK signaling. To test this, we comparatively analyzed between parental 293T and 293T<sup>CIC</sup> cells the dynamic *DUSP6* expression profiles in response to alteration of ERK signaling. In parental 293T cells, expression of *DUSP6* correlated well with the activity of ERK signaling, i.e., rise when ERK signaling is stimulated by FGF and drop when ERK signaling is blocked by an ERK inhibitor, SCH772984. By contrast, *DUSP6*

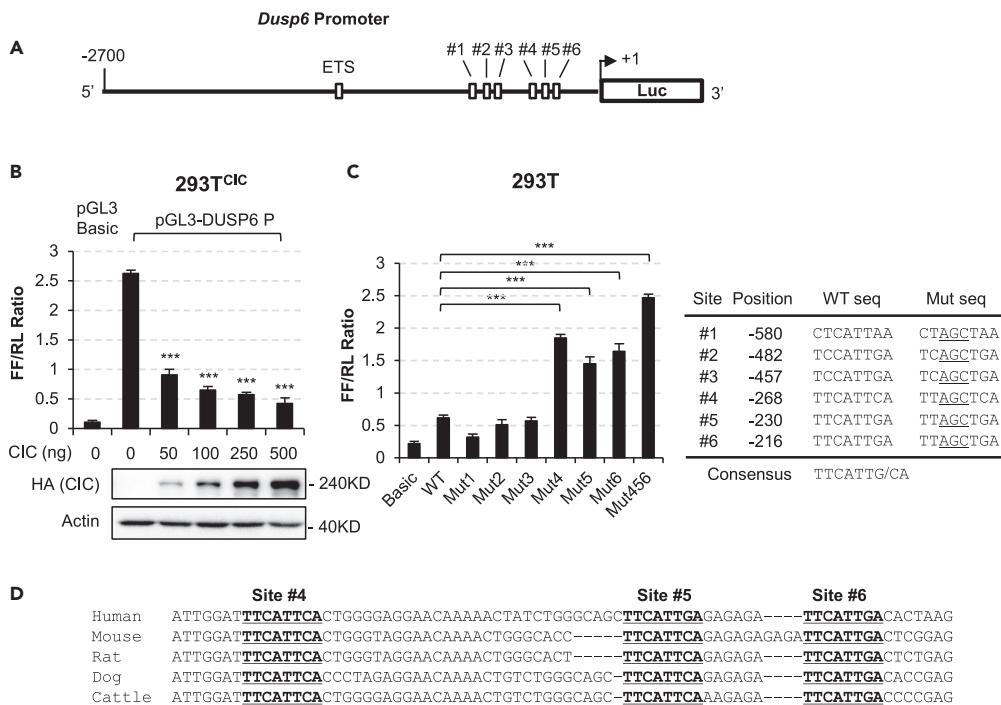


**Figure 2. CIC Represses DUSP6 Promoter Activity Through Three CREs**

(A) A schematic diagram of the DUSP6 promoter-luciferase reporter construct with the known regulatory ETS1 binding site and six putative CIC-binding sites shown.

(B) 293T<sup>CIC</sup> cells were transfected with 500 ng pGL3-DUSP6 P (or pGL3-Basic as negative control), 50 ng pRL-TK and a titration of HA-CIC expressing plasmids. After 48 h, cells were lysed and dual-luciferase reporter assays were performed. Data are represented as mean  $\pm$  SEM (N = 3). The expression of exogenous HA-CIC was verified by western blot. Significance was determined by one-way ANOVA test, \*\*\*p < 0.001.

(C) 293T cells were co-transfected with 500 ng pGL3-DUSP6 promoter constructs with either WT promoter sequence or mutations in the six putative CIC-binding sites, 50 ng pRL-TK and 500 ng HA-CIC expressing plasmid for 48 h. Data were analyzed as in (B), \*\*\*p < 0.001. Mutations of CIC-binding sites were shown on the right with substituted nucleotides underlined. The consensus motif "TTCATTG/CA" is a reverse complementary sequence of previously reported consensus (Ajuria et al., 2011; Jimenez et al., 2000; Weissmann et al., 2018).

(D) Sequence alignment of CIC-binding sites in DUSP6 promoters of different species. The CIC-binding sites were shown in bold and underlined.

expression was much less sensitive to changes in ERK signaling activity in CIC-depleted cells, especially when ERK signaling is inhibited (Figure 1E). Similarly, the decreasing of DUSP6 expression upon ERK signaling blockade was more prominent in MCF7 than in MCF7<sup>CIC</sup> cells (Figure 1F). To further validate these results, we used specific siRNAs to knockdown CIC in a melanoma cell line 1205Lu, which has constitutively active ERK signaling due to the presence of a BRAF<sup>V600E</sup> mutation (Davies et al., 2002). Inhibition of ERK signaling (by a RAF inhibitor, PLX4032) in 1205Lu cells led to a time-dependent decrease of DUSP6 expression. CIC knockdown, however, conspicuously slowed down the decline of DUSP6 expression (Figure 1G). The impacts of CIC siRNAs on DUSP6 expression were correlated with their knockdown efficiencies (Figure 1G). Together, the above results strongly supported the notion that CIC mediates the regulation of DUSP6 by ERK signaling as a transcriptional repressor.

### CIC Inhibits the Transcription of DUSP6 Promoter through Multiple CREs

We next constructed DUSP6 promoter reporter plasmid to assay for the impact of CIC on its transcriptional activity (Figure 2A). In 293T<sup>CIC</sup> cells, DUSP6 promoter exhibited robust transcription activity when compared with the empty vector control (Figure 2B). Reintroduction of exogenous CIC dose dependently inhibited DUSP6 promoter activity, reinforced the conclusion that CIC functions as a transcription repressor of DUSP6 (Figure 2B). Using bioinformatical analysis, we discovered in the DUSP6 promoter region six putative CIC-binding sites (sites #1–#6) that match the octameric consensus binding motif (TTCATTG/CA) of CIC (Figure 2A). Individually mutating sites #1, #2, or #3 had only mild influences on the transcription activity

of DUSP6 promoter in wild-type (WT) 293T cells, which express endogenous CIC (Figure 2C). By contrast, mutation of sites #4, #5, or #6 alone led to significant derepression of DUSP6 promoter (Figure 2C). Concurrent disruption of sites #4–#6 further enhanced promoter activity. These results demonstrated that sites #4, #5, #6, instead of sites #1, #2, #3, are mostly likely responsible for the transcription repression of DUSP6 promoter by CIC. Of note, sites #4, #5, #6 (but not sites #1, #2, #3) are evolutionally conserved among different species (Figure 2D).

### CIC Directly Binds to CREs in DUSP6 Promoter

Unlike other HMG family DNA-binding proteins, CIC recognizes its DNA target through a collaborative action of the HMG domain and C-terminal C1 domain (Fores et al., 2017). To investigate whether CIC acts directly on the CREs identified in DUSP6 promoter, we purified CIC-HMG domain only and CIC-HMG/C1 fusion protein (Figure 3A) and probed their bindings with DNA fragments containing sites #4, #5, and #6, respectively. Isothermal titration calorimetry analysis revealed that CIC HMG/C1 fusion protein bound to three sites with similar affinities, but the HMG domain showed no binding (Figure S2). The CIC HMG/C1-DNA interactions were further confirmed by independent EMSA experiments (Figure 3B). Mutation of the CIC-binding site #4 abolished the recognition of the corresponding DNA fragment by CIC HMG/C1, indicating the binding was specific (Figure 3C). We next performed ChIP analysis to investigate whether CIC binds to the CREs within DUSP6 promoter *in vivo*. Since the three CIC-binding sites (#4–#6) are positioned very close to each other (within 150 bp), we designed one pair of primers to detect the binding of endogenous CIC to a region spanning all three sites in parental 293T and MCF7 cells (Figure 3D). Although no enrichment was detected in CIC versus IgG immunoprecipitates on a genomic region between the GAPDH and CNAP1 genes (served as negative control), the region containing three CIC-binding sites was significantly enriched in CIC immunoprecipitates versus the IgG control (Figure 3D), indicating CIC indeed binds to the CREs in DUSP6 promoter *in vivo*.

### ERK/p90RSK Signaling Controls CIC Repressor Activity on DUSP6 by Regulating Its Nucleus/Cytoplasm Distribution

Since CIC mediates the transcriptional regulation of DUSP6 by ERK signaling and CIC itself directly represses DUSP6 transcription, we ask whether ERK signaling controls the repressor activity of CIC on DUSP6. To test this, we conducted dual luciferase assays on DUSP6 promoter reporter in 293T<sup>CIC</sup> cells with altered ERK signaling. Meanwhile, an ERK-regulated transcription factor ETS1 has been reported to activate DUSP6 transcription through direct promoter binding (Ekerot et al., 2008) (Figure 2A). We therefore mutated this ETS1 site in DUSP6 promoter so that the effects of altered ERK signaling on CIC's repressive activity toward DUSP6 can be assessed without interference from ETS. Consistent with prior observations, overexpression of exogenous CIC potentially inhibited DUSP6 promoter activity in 293T<sup>CIC</sup> cells (Figure 4A). When co-expressed with BRAF<sup>V600E</sup>, a mutant BRAF variant that hyperactivates the MEK/ERK1/2 signaling (Davies et al., 2002), the transcription repression activity of CIC was greatly diminished, indicating ERK signaling negatively regulates CIC repressor activity toward DUSP6 (Figures 4A and 4B). To further support this, we found inhibition of BRAF<sup>V600E</sup>-hyperactivated ERK signaling with a MEK inhibitor AZD6244 effectively restored the repression of DUSP6 promoter by CIC (Figures 4A and 4B). Interestingly, inhibition of the ERK-downstream kinase p90RSK with an inhibitor LJM685 also rescued CIC-mediated repression of DUSP6 promoter (Figures 4A and 4B). Of note, the p90RSK inhibitor did not reduce the levels of activated ERK1/2 (Figure 4B), indicating that p90RSK, rather than ERK1/2 is most likely the immediate upstream regulator of CIC.

How does the ERK/p90RSK signaling control CIC's repressor activity toward DUSP6 then? Modulation of the MAPK pathway activity either by mitogen stimulation in 293T or MCF7 cells (Figure S3) or by RAF inhibitor treatment in the mutant BRAF melanoma cell line 1205Lu (Figure 1G) did not alter endogenous CIC protein levels at least within 12 h. Therefore, we wondered whether ERK/p90RSK signaling would possibly regulate the function of CIC by altering its nucleus/cytoplasm distribution. In the absence of mitogen stimulation, CIC preferably located in the nucleus presumably owing to its nuclear localization sequence (NLS) (Dissanayake et al., 2011). FGF or EGF stimulation resulted in a time-dependent increase in the cytosolic fraction of CIC and a concomitant drop of the nuclear fraction in both 293T and MCF7 cells (Figures 4C–4F, 4H, and S4). On the contrary, inhibition of ERK1/2 or p90RSK led to a decrease in the cytosolic pool of CIC, whereas an increase in the nuclear counterpart (Figures 4G and 4H). These results suggested that the ERK/p90RSK signaling likely controls CIC's repressor activity toward DUSP6 through regulating its nucleus/cytoplasm distribution.

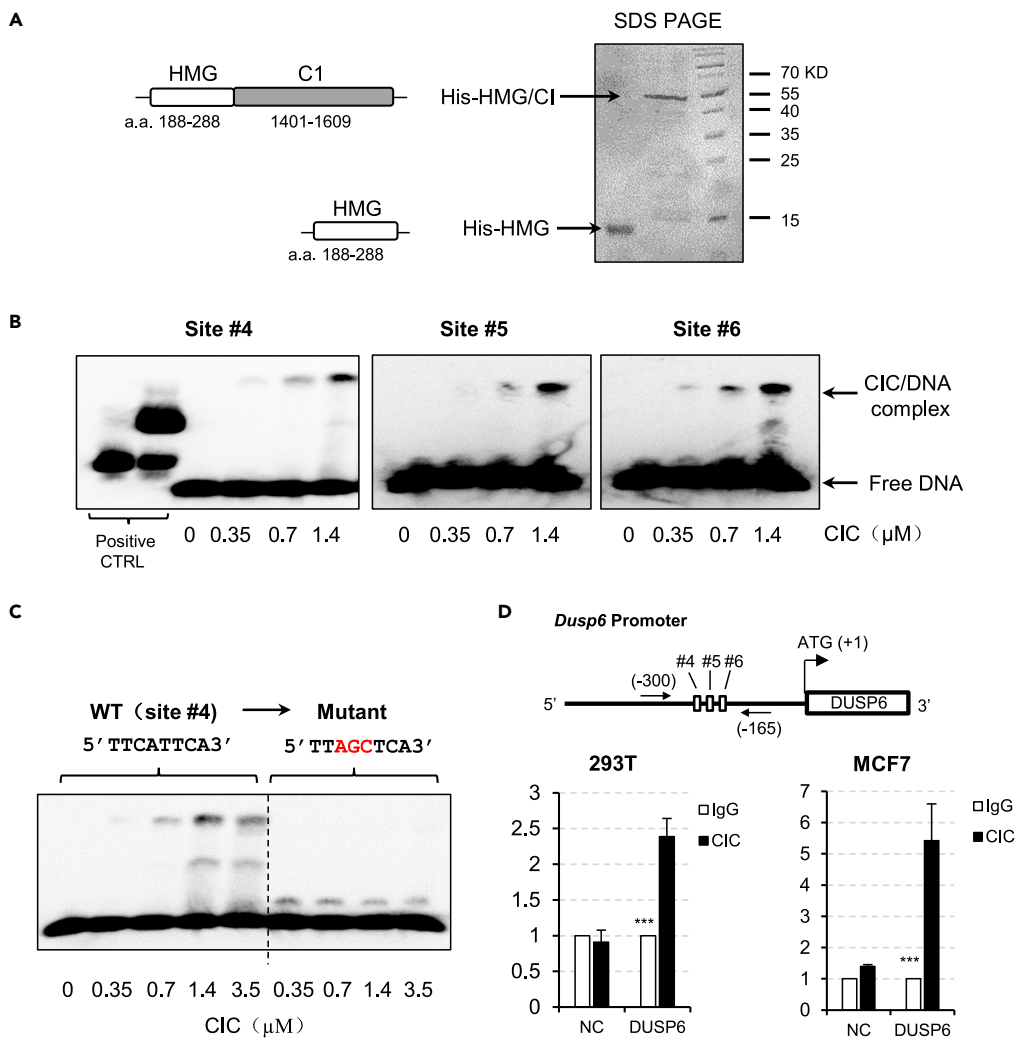


**Figure 3. CIC Directly Binds to the CREs of DUSP6 Promoter In Vitro and In Vivo**

(A) Schematic shows CIC-HMG/C1 and CIC-HMG proteins (left) and SDS PAGE of purified recombinant CIC proteins (right).

(B) EMSA assays probing the interaction of CIC-HMG/C1 fusion protein with DUSP6 CREs. Positive control: binding of EBV nuclear antigen (EBNA) to its cognate DNA target.

(C) Comparative analysis of the binding of CIC-HMG/C1 fusion protein to site #4 or its mutant analog.

(D) ChIP analysis of CIC binding to the DUSP6 promoter was performed in 293T and MCF7 cells. Top: Schematic diagram of DUSP6 promoter region with CIC-binding sites #4, #5, #6 and ChIP primers shown; Bottom: quantitation of ChIP analysis results. Occupancy of CIC on a region spanning sites #4–#6 in DUSP6 promoter and a region between the GAPDH and CNAP1 genes (negative control, NC) was evaluated. Data are represented as mean  $\pm$  SEM (N = 3). Significance was determined by one-way ANOVA test, \*\*\*p < 0.001.

See also [Figure S2](#).

### p90RSK Regulates CIC Nucleus/Cytoplasm Distribution through Direct Phosphorylation

Cellular fractionation and immunofluorescence studies revealed that CIC rapidly translocates from nucleus into cytoplasm upon mitogen stimulation and p90RSK inhibitor can block this process ([Figure 4](#)). We thus asked whether p90RSK regulates CIC's cellular localization through direct phosphorylation. Bioinformatical analysis of CIC's protein sequence revealed two potential p90RSK phosphorylation sites that match the consensus motif "R/KXRXXS/T." Interestingly, these two sites straddle the HMG DNA-binding domain of CIC and show high level of evolutionary conservation ([Figure 5A](#)). Using multiple reactions monitoring (MRM) mass spectrometry, we detected phosphorylation of ectopically expressed HA-CIC at S173 and S301 sites in 293T<sup>CIC</sup> cells ([Figure 5B](#)). FGF treatment further enhanced the phosphorylation levels of these

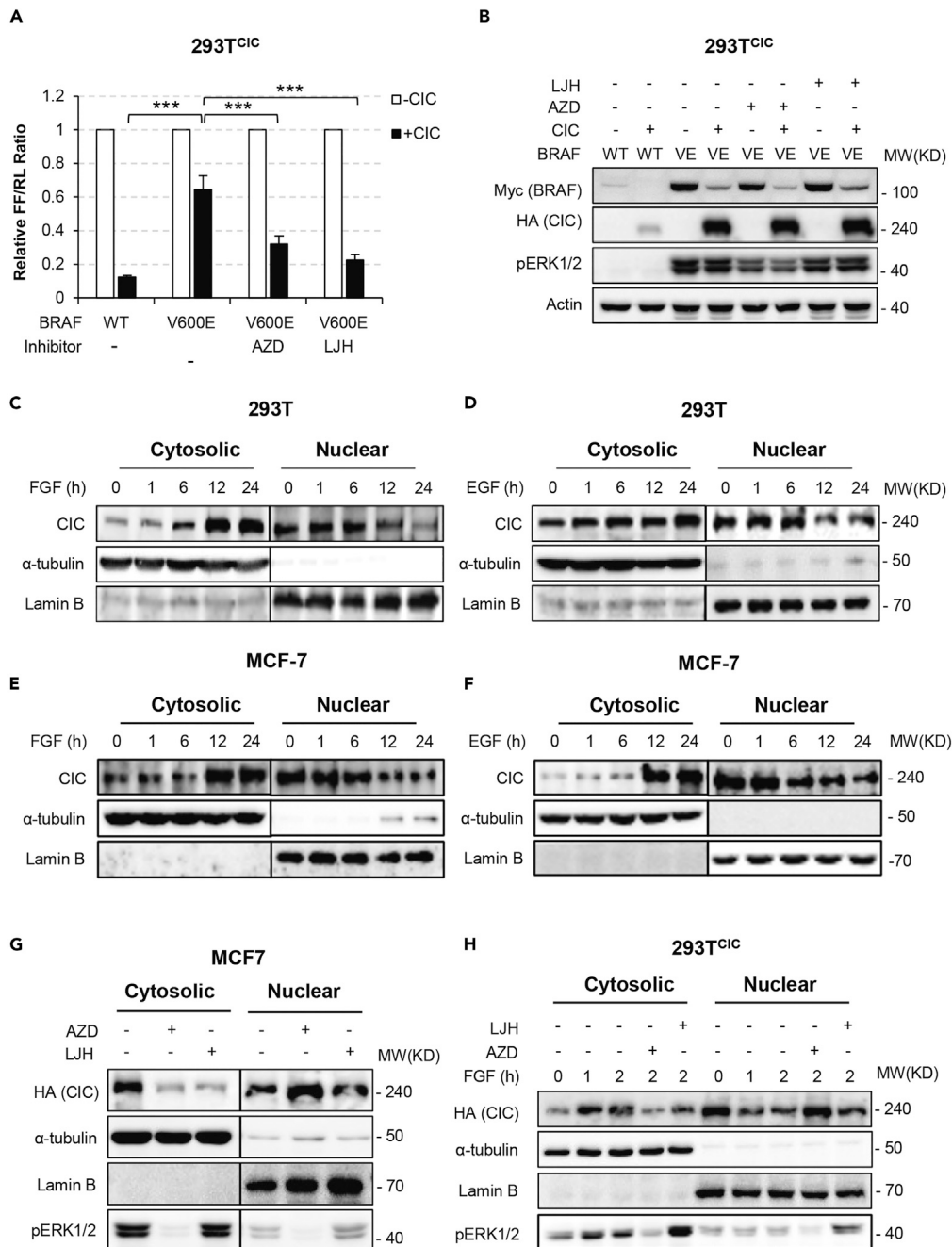


**Figure 4. ERK1/2/p90RSK Signaling Regulates the Subcellular Distribution of CIC**

(A) 293T<sup>CIC</sup> cells were co-transfected with pGL3-DUSP6 reporter construct, pRL-TK, Myc-tagged BRAF<sup>WT</sup>, or BRAF<sup>V600E</sup> plasmids, +/- HA-CIC plasmid. After 48 h, cells were treated with or without MEK inhibitor, AZD6244 (10 μM) or p90RSK inhibitor, LJH658 (10 μM) for 4 h and lysed for dual-luciferase assay. Data are represented as mean ± SEM (N = 3). Significance was determined by ANOVA one-way test, \*\*\*p < 0.001.

(B) 293T<sup>CIC</sup> cells were treated as in (A) and lysed for western blot analysis.

(C–D) 293T cells were treated with 10 ng/mL FGF (C) or 75 ng/mL EGF (D) for indicated time points and then subjected to nuclear/cytoplasmic fractionation and western blot analysis.

(E–F) MCF7 cells were treated with 10 ng/mL FGF (E) or 75 ng/mL EGF (F) for indicated time points and then subjected to nuclear/cytoplasmic fractionation and western blot analysis.

(G) MCF7 cells transfected with HA-CIC expressing plasmid (48 h) were treated with 10 μM AZD6244 or 10 μM LJH658 for 3 h. Cells were then subjected to nuclear/cytoplasmic fractionation and western blot analysis.

**Figure 4. Continued**

(H) 293T<sup>CIC</sup> cells were transfected with HA-CIC expressing plasmid for 48 h and treated with -/+FGF, -/+AZD6244, and -/+LJH658 as indicated. Cells were then subjected to nuclear/cytoplasmic fractionation and western blot analysis. See also Figures S3 and S4.

two sites (Figures 5B and 5C). We then performed *in vitro* kinase assay using recombinant activated p90RSK and an extended CIC-HMG domain that harbors the two phosphorylation sites (aa 156–330). As shown in Figure 5D, WT CIC-HMG was successfully phosphorylated by p90RSK. By comparison, S173A or S301A CIC-HMG showed reduced phosphorylation and the S173A/S301A (AA) double mutant was least phosphorylated (Figure 5D). These results demonstrated that p90RSK can directly phosphorylate CIC at S173 and S301. We then tested whether S173/S301 phosphorylation would interfere with CIC's nucleus/cytoplasm translocation using cellular fractionation experiments. Consistent with prior observation, WT HA-CIC rapidly relocalized from nucleus to cytoplasm when cells were stimulated with FGF (Figure 5E). Of note, S173A, S301A, or AA mutations blocked FGF-stimulated cytoplasmic translocation of CIC and rendered CIC's repressor activity on DUSP6 irresponsive to FGF stimulation (Figures 5E and 5F). Together, these results indicated that phosphorylation of CIC at S173 and/or S301 is required for its nuclear export and for derepression of DUSP6 transcription.

**S173/S301 Phosphorylation Promotes CIC Nuclear Export through 14-3-3 Binding**

The 14-3-3 family proteins bind as a dimer to a variety of phosphorylated protein targets through interacting simultaneously with two "RXXpS/T" phospho-motifs within target proteins and sequester them in the cytoplasm. Since phosphorylation of S173 and S301 by p90RSK creates two sites that match the 14-3-3 recognition motif, we postulated that the phosphorylation of these two sites may result in CIC nuclear export through 14-3-3 binding. To test this, we first interrogated the interaction between recombinant 14-3-3 protein and phosphorylated CIC peptides using isothermal titration calorimetry (Figure 6A). Indeed, 14-3-3 protein bound pS173 or pS301 CIC peptides with micromolar-range affinities but showed undetectable binding with the non-phosphorylated control peptides. We then performed a pull-down assay using purified 14-3-3 protein and lysates of 293T<sup>CIC</sup> cells expressing exogenous HA-CIC. As shown in Figure S5, 14-3-3 successfully pulled down HA-CIC from the lysates. Of note, FGF stimulation strengthened 14-3-3/HA-CIC interaction while inhibition of p90RSK weakened the binding between 14-3-3 and HA-CIC. To further understand the details of 14-3-3/CIC interaction at atomic level, we solved the crystal structure of 14-3-3 $\theta$  in complex with each individual CIC phospho-peptide at high resolution (Figure 6B and Table S1). The 14-3-3 $\theta$  protein complexes with CIC phospho-peptides in a classic mode where two 14-3-3 $\theta$  molecules assemble into a dimer through the N-terminal dimerization interface and each CIC phospho-peptide occupies one canonical ligand binding groove of the 14-3-3 $\theta$  dimer as shown by the electron density mapping (Figures 6B–6D). The pS301 and pS173 peptides interact with 14-3-3 $\theta$  protein in a very similar way, employing nine and eight hydrogen bonds, respectively (Figures 6E and 6F). In both cases, the phosphorylated serine is immobilized through five hydrogen bonds formed with a conserved Arg56-Arg127-Tyr128 triad from 14-3-3 $\theta$  protein. Two additional hydrogen bonds, one between Asn173 of 14-3-3 $\theta$  and the +1 backbone of the peptide (relative to the phosphoserine), the other between Asn224 of 14-3-3 $\theta$  and the -1 backbone of the peptide, further stabilize the 14-3-3 $\theta$ /CIC peptide complex. Interestingly, in the complex of 14-3-3 $\theta$ /CIC pS301, one more hydrogen bond is observed between Trp228 from 14-3-3 $\theta$  and Ser299 in the CIC peptide. In summary, our biochemical and structural studies consistently demonstrated that S173/S301-phosphorylated CIC peptides can interact with 14-3-3 protein in a canonical fashion.

**The CIC-DUX4 Fusion Oncoprotein Is an Activator of DUSP6 and Remains Regulated by ERK Signaling**

CIC-DUX4 is a fusion oncoprotein frequently found in small round cell sarcoma (Kawamura-Saito et al., 2006; Okimoto et al., 2019; Yoshimoto et al., 2017). Although CIC-DUX4 retained the majority of CIC gene, fusion with DUX4 turned CIC from a transcription repressor into an activator of the PEA3 family genes (Kawamura-Saito et al., 2006). We thus compared the regulatory effects of native CIC and CIC-DUX4 on DUSP6 expression. Native CIC expectedly inhibited DUSP6 expression in 293T<sup>CIC</sup> cells, but CIC-DUX4 activated DUSP6 expression (Figure 7A). Importantly, we found that FGF stimulation could still induce the translocation of CIC-DUX from nucleus to cytoplasm (Figure 7B), indicating that the ERK/p90RSK-dependent regulatory circuit remained intact in CIC-DUX4 even when it turned from a repressor into an activator.

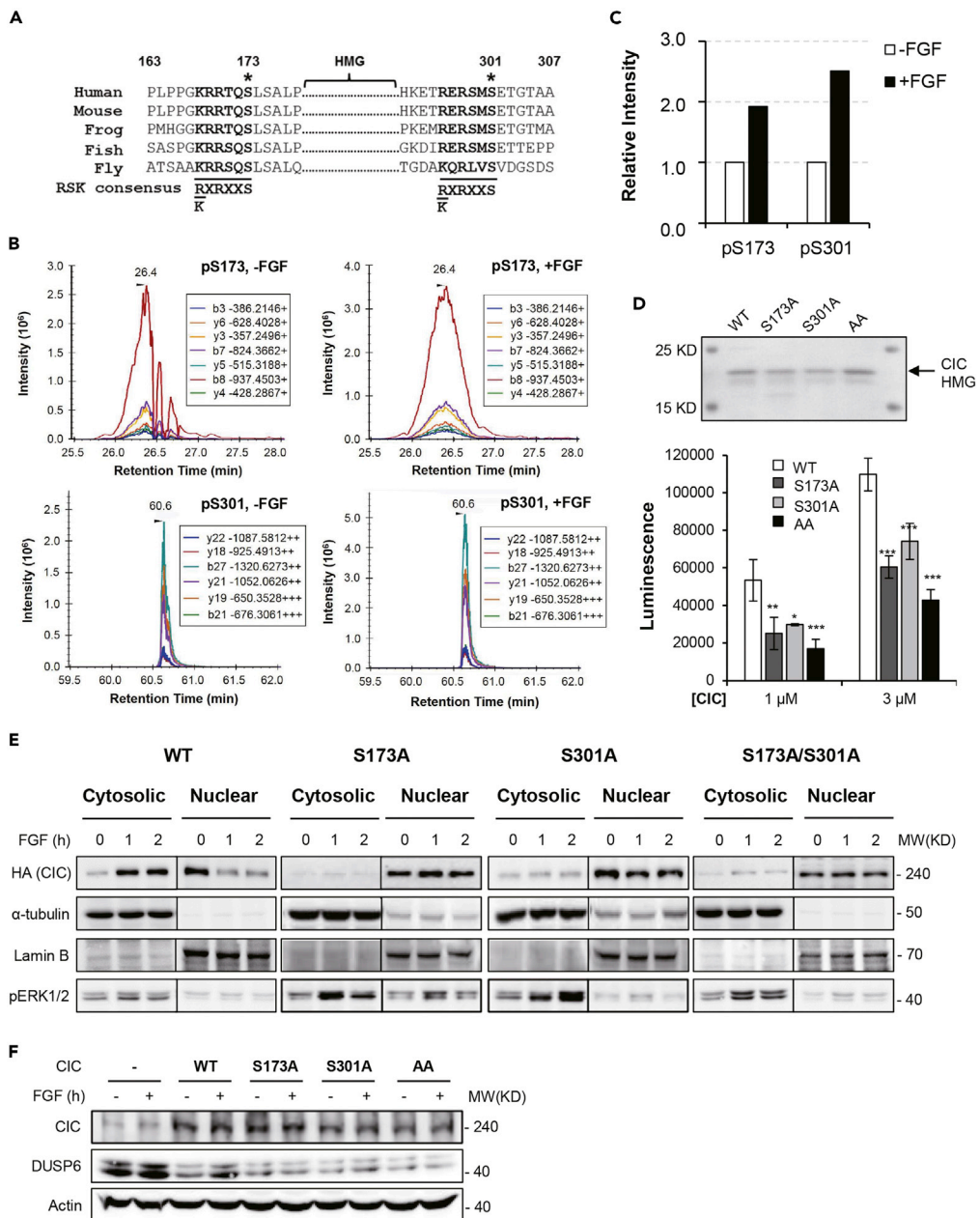


**Figure 5. p90RSK Regulates CIC Subcellular Distribution through Directly Phosphorylating CIC at S173 and S301 Sites**

(A) Sequence alignment of the putative p90RSK phosphorylation motifs in CIC from different species.

(B) *In vivo* detection of CIC phosphorylation at S173 and S301. 293T<sup>CIC</sup> cells were transfected with HA-CIC plasmid for 48 h and treated with  $-/+$  10 ng/mL FGF for 4 h. Cells were lysed and HA-CIC were immunoprecipitated, digested by trypsin, and analyzed by multiple reactions monitoring (MRM) mass spectrometry. MRM spectra of S173- and S301-phosphorylated CIC tryptic fragments are shown.

(C) Quantitation of CIC phosphorylation in 293T<sup>CIC</sup> cells treated with or without FGF. The areas of the peptide peaks in MRM chromatograms were measured to estimate the relative quantities of corresponding peptides.

(D) *In vitro* kinase assay was carried out using purified CIC fragments and activated recombinant GST-p90RSK. Top: SDS PAGE of purified WT CIC HMG domain (expanded to include the two phosphorylation sites) and its mutant analogs. Bottom: quantitation of the luminescence as an indicator of phosphorylation level. Data are represented as mean  $\pm$  SEM (N = 3). Significance was determined by ANOVA one-way test, \*p < 0.05, \*\*p < 0.01, \*\*\*p < 0.001.

**Figure 5. Continued**

(E) 293T<sup>CIC</sup> cells were transfected with WT, S173A, S301A, or AA HA-CIC plasmids for 48 h and treated with 10 ng/mL FGF for 0, 1, 2 h. Cells were then subjected to nuclear/cytoplasmic fractionation and western blot analysis.

(F) 293T<sup>CIC</sup> or lentivirus-transduced 293T<sup>CIC</sup> cells (expressing exogenous WT, S173A, S301A, or AA CIC) were treated with 10 ng/mL FGF for 6 h and analyzed by western blotting.

**DISCUSSION**

The reciprocal regulation of ERK1/2 and DUSP6 constitutes an important negative feedback circuit to keep ERK1/2 pathway activity within physiological range. Although DUSP6 ostensibly inactivates ERK1/2 through direct dephosphorylation, how ERK1/2 signaling rapidly and dynamically regulates DUSP6 expression is not fully understood. Response of DUSP6 transcription to mitogen stimulation or ERK1/2 signaling blockade takes place within hours (Ekerot et al., 2008; Packer et al., 2009), implying the presence of mediating transcriptional factors that can be quickly turned on and off by post-translational modification. Indeed, one of the ERK1/2-responsive transcription factor, ETS1, has been found to positively regulate DUSP6 transcription by direct promoter binding (Ekerot et al., 2008; Zhang et al., 2010). In this study, we identified CIC as a new regulator of DUSP6 transcription downstream of ERK1/2 signaling. In contrast to ETS1, CIC acts on DUSP6 transcription in a default repression fashion and this repression can be relieved by the ERK1/2 downstream kinase, p90RSK, which phosphorylates CIC and causes nuclear export of CIC. It is speculated that this dual-mode regulation of DUSP6 by ETS1 and CIC ensures the rapid and tight control of DUSP6 by the ERK1/2 signaling (see Graphic Abstract).

How does RTK/MAPK signaling regulate CIC's repressor activity? In *Drosophila*, the Torso signaling promotes CIC degradation through post-translational modification and EGFR signaling regulates its subcellular distribution (Astigarraga et al., 2007; Jimenez et al., 2000). In mammalian cells, the regulation of CIC activity by RTK/MAPK signaling appears less well characterized. Dissanayake et al. proposed a model in melanoma cells that p90RSK phosphorylates CIC at S173 within the HMG DNA-binding domain, which recruits 14-3-3 binding to the HMG domain and blocks its DNA binding (Dissanayake et al., 2011). Intriguing as it is, there are still several uncertainties regarding this model: (1) 14-3-3 proteins usually bind as dimer to their targets, but the second CIC phosphorylation site required for 14-3-3 recognition was missing in this model; (2) the proposed mode of 14-3-3 action, i.e., to block the DNA binding of CIC, may require further validation because the DNA binding ability of CIC was tested using a CIC fragment harboring the HMG domain only, whereas studies from Fores et al. clearly demonstrated that the presence of both HMG and C1 domains are essential for CIC's DNA binding (Fores et al., 2017). Our work provided substantial evidence for a revised model of CIC regulation by ERK1/2/p90RSK signaling. In this model, p90RSK phosphorylates both S173 and S301 of CIC, creating an optimal recognition motif for 14-3-3. Binding of 14-3-3 to CIC, instead of interfering with DNA binding by CIC, causes nuclear export of CIC and therefore inhibits its transcriptional repressor activity (see Graphic Abstract). Importantly, the binding of phosphorylated-CIC peptides (pS173 or pS301) to 14-3-3 was confirmed by our biochemical and crystallographic studies. Nevertheless, it is still possible that the differences observed between the two studies may stem from different cellular contexts.

The CIC-DUX4 fusion protein is implicated in the metastasis and tumorigenesis of small round cell sarcomas (Okimoto et al., 2019). Mechanistic studies revealed that CIC-DUX4 drives the development of sarcoma by activating the *PEA3* family genes (Kawamura-Saito et al., 2006). In this study, we found that CIC-DUX4 activated, instead of repressing, DUSP6 expression, whereas the subcellular localization of CIC-DUX4 was still regulated by the ERK signaling. This reversal of transcriptional activity toward DUSP6 would intriguingly turn the ERK/CIC/DUSP6 negative feedback loop into a more positive feedback-like circuit where CIC-DUX4 induces overexpression of DUSP6, which would tune down the ERK signaling, thereby promoting nuclear localization of CIC-DUX4 and subsequent transcription of target genes such as *DUSP6* and the *PEA3* family genes. Indeed, this ERK/CIC-DUX4/DUSP6 feedforward circuit has been recently confirmed in sarcoma and DUSP6 inhibition appears to be a promising therapeutic approach to target CIC-fused sarcoma (Lin et al., 2020). It will be of interest to further evaluate the expression of DUSP6 in CIC-DUX4 sarcoma samples and its correlation with disease prognosis.

In summary, this work completes an ERK1/2/p90RSK/CIC/DUSP6 negative feedback circuit and elucidates the molecular mechanism of CIC's regulation by ERK signaling in mammalian cells.

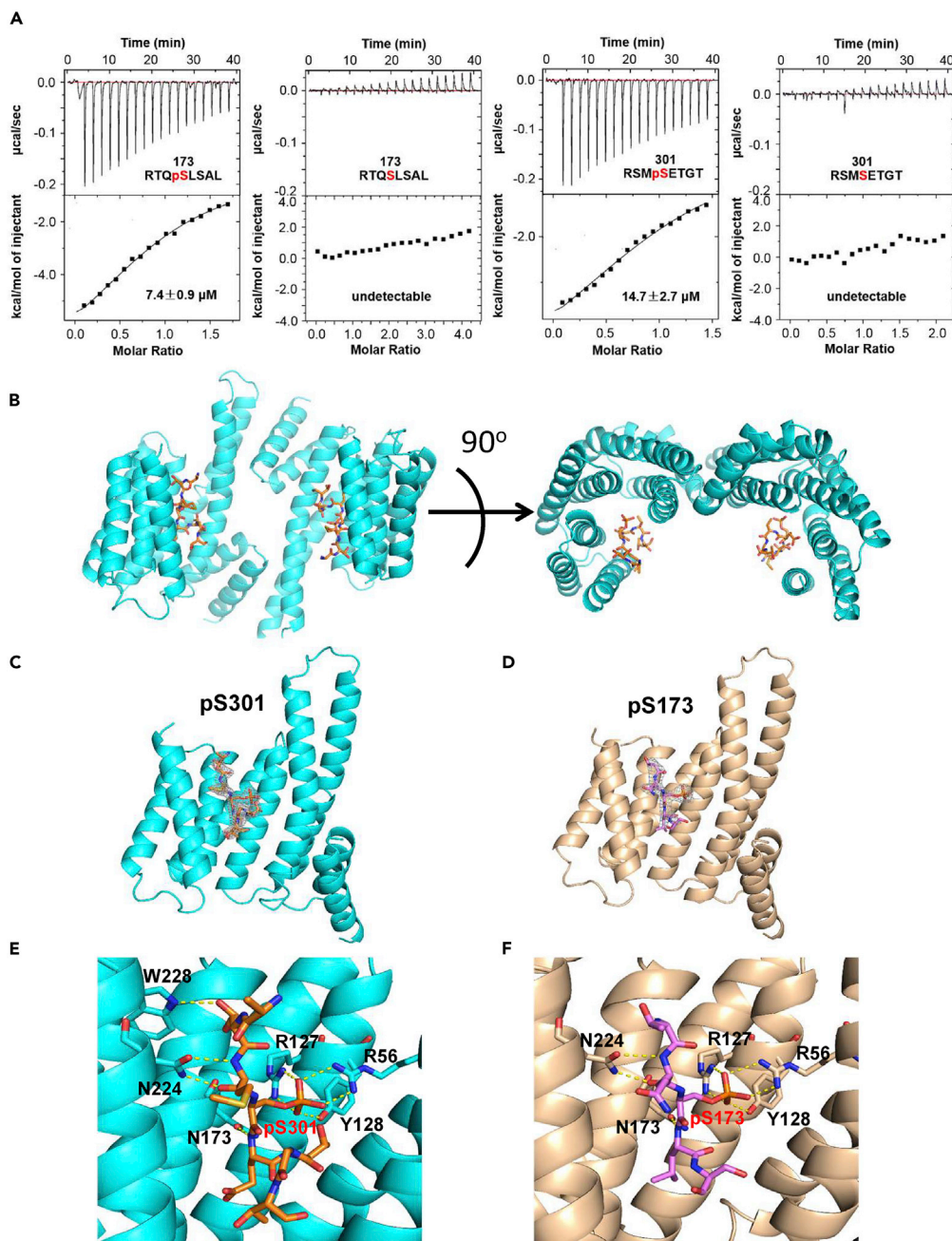


**Figure 6. S173/S301 Phosphorylation Promotes CIC/14-3-3 Interaction**

(A) ITC analysis of interaction between 14-3-30 and S173/S301-phosphorylated or non-phosphorylated CIC peptides. (B) Overall crystal structure of 14-3-30/pS173 CIC peptide dimer complex, the CIC peptide occupies the canonical binding groove of the 14-3-30 protein, which assembles into dimer through the N-terminal dimerization interface. (C and D) The electron density maps of pS301(C) and pS173(D) peptides in the binding groove of 14-3-30 shown in 2Fo-Fc at  $2\sigma$  and  $1.5\sigma$ , respectively. (E and F) The detailed interaction interfaces between pS301 (E) or pS173 (F) peptide and 14-3-30 protein. The phosphate groups of the pS301 and pS173 were anchored with the conserved Arg56, Arg127, and Tyr128, and the interactions were further stabilized by hydrogen bonds between Asn224, Asn173 of 14-3-30 and -1, +1 backbone atoms of the peptide, respectively. One additional hydrogen bond was observed between 14-3-30 W228 and pS301 CIC peptide. See also [Figure S5](#) and [Table S1](#).

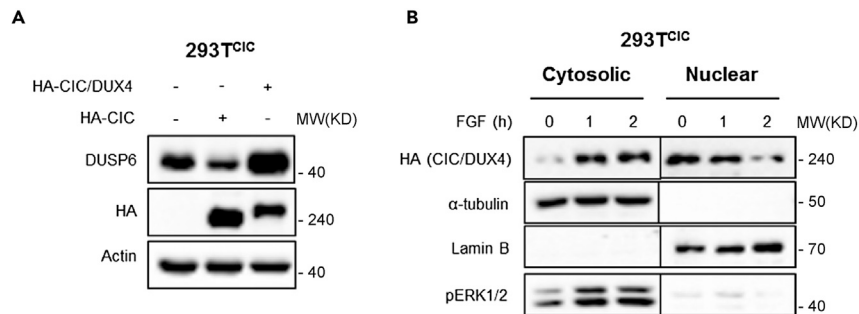


**Figure 7. CIC/DUX Fusion Protein is an Activator of DUSP6 and Remains Regulated by ERK Signaling**

(A) 293T<sup>CIC</sup> cells were transfected with empty control, HA-CIC, or HA-CIC/DUX4-expressing plasmids for 48 h. Cells were lysed for western blot analysis on indicated proteins.

(B) 293T<sup>CIC</sup> cells were transfected with HA-CIC/DUX4 plasmids for 48 h and treated with FGF for 0, 1, 2 h. Cells were harvested and subjected to cytoplasmic/nuclear fractionation followed by western blot analysis.

### Limitations of the Study

This study characterized a CIC-mediated transcriptional feedback circuit of the ERK signaling in mammalian cells. However, the *in vivo* significance of this regulatory circuit remains to be tested.

### Resource Availability

#### Lead Contact

Further requests should be directed to and will be fulfilled by the lead contact Dr. Yongping Shao ([yongping.shao@mail.xjtu.edu.cn](mailto:yongping.shao@mail.xjtu.edu.cn)).

#### Materials Availability

Materials are available upon reasonable request.

#### Data and Code Availability

The crystallography data have been deposited to the Protein Data Bank (<http://www.pdb.org>). PDB: 6KZG, 6KZH.

## METHODS

All methods can be found in the accompanying [Transparent Methods supplemental file](#).

## SUPPLEMENTAL INFORMATION

Supplemental Information can be found online at <https://doi.org/10.1016/j.isci.2020.101635>.

## ACKNOWLEDGMENT

The 1205Lu cells were kindly gifted by Dr. Meenhard Herlyn at the Wistar Institute. This work was supported by the National Natural Science Foundation of China (31970724, 31771557 to Y.S., 82072237, 31870132 to Y.W.). We thank the staffs from BL18U1/BL19U1 beamline for technical support during data collection in National Center for Protein Sciences Shanghai (NCPSS) at Shanghai Synchrotron Radiation Facility.

## AUTHOR CONTRIBUTIONS

Y.S. conceived and designed the research. Y.R., Z.O., Z.H., Y.Y., Z.Z., M.S., M.D., and H.L. performed the research. Y.R., Z.O., Z.H., H.L., Y.W., and Y.S. analyzed the data. Y.S., Y.R., and Y.W. wrote the manuscript, and all authors reviewed and approved the manuscript for publication.

## DECLARATION OF INTERESTS

The authors declare no conflict of interest.

Received: December 4, 2019

Revised: September 1, 2020

Accepted: September 29, 2020

Published: November 20, 2020

## REFERENCES

- Ajuria, L., Nieva, C., Winkler, C., Kuo, D., Samper, N., Andreu, M.J., Helman, A., Gonzalez-Crespo, S., Paroush, Z., Courey, A.J., et al. (2011). Capicua DNA-binding sites are general response elements for RTK signaling in *Drosophila*. *Development* 138, 915–924.
- Astigarraga, S., Grossman, R., Diaz-Delfin, J., Caelles, C., Paroush, Z., and Jimenez, G. (2007). A MAPK docking site is critical for downregulation of Capicua by Torso and EGFR RTK signaling. *EMBO J.* 26, 668–677.
- Chang, L., and Karin, M. (2001). Mammalian MAP kinase signalling cascades. *Nature* 410, 37–40.
- Davies, H., Bignell, G.R., Cox, C., Stephens, P., Edkins, S., Clegg, S., Teague, J., Woffendin, H., Garnett, M.J., Bottomley, W., et al. (2002). Mutations of the BRAF gene in human cancer. *Nature* 417, 949–954.
- Dhillon, A.S., Hagan, S., Rath, O., and Kolch, W. (2007). MAP kinase signalling pathways in cancer. *Oncogene* 26, 3279–3290.
- Dissanayake, K., Toth, R., Blakey, J., Olsson, O., Campbell, D.G., Prescott, A.R., and MacKintosh, C. (2011). ERK/p90(RSK)/14-3-3 signalling has an impact on expression of PEA3 Ets transcription factors via the transcriptional repressor capicua. *Biochem. J.* 433, 515–525.
- Ekerot, M., Stavridis, M.P., Delavaine, L., Mitchell, M.P., Staples, C., Owens, D.M., Keenan, I.D., Dickinson, R.J., Storey, K.G., and Keyse, S.M. (2008). Negative-feedback regulation of FGF signalling by DUSP6/MKP-3 is driven by ERK1/2 and mediated by Ets factor binding to a conserved site within the DUSP6/MKP-3 gene promoter. *Biochem. J.* 412, 287–298.
- Fores, M., Ajuria, L., Samper, N., Astigarraga, S., Nieva, C., Grossman, R., Gonzalez-Crespo, S., Paroush, Z., and Jimenez, G. (2015). Origins of context-dependent gene repression by capicua. *PLoS Genet.* 11, e1004902.
- Fores, M., Simon-Carrasco, L., Ajuria, L., Samper, N., Gonzalez-Crespo, S., Drost, M., Barbacid, M., and Jimenez, G. (2017). A new mode of DNA binding distinguishes Capicua from other HMG-box factors and explains its mutation patterns in cancer. *PLoS Genet.* 13, e1006622.
- Gleize, V., Alentorn, A., Connen de Kerillis, L., Labussiere, M., Nadaradjane, A.A., Mundwiller, E., Ottolenghi, C., Mangesius, S., Rahimian, A., Ducray, F., et al. (2015). CIC inactivating mutations identify aggressive subset of 1p19q codeleted gliomas. *Ann. Neurol.* 78, 355–374.
- Huang, C.Y., and Tan, T.H. (2012). DUSPs, to MAP kinases and beyond. *Cell Biosci.* 2, 24.
- Jennings, B.H., and Ish-Horowicz, D. (2008). The Groucho/TLE/Grg family of transcriptional co-repressors. *Genome Biol.* 9, 205.
- Jimenez, G., Guichet, A., Ephrussi, A., and Casanova, J. (2000). Relief of gene repression by torso RTK signaling: role of capicua in *Drosophila* terminal and dorsoventral patterning. *Genes Dev.* 14, 224–231.
- Johnson, G.L., and Lapadat, R. (2002). Mitogen-activated protein kinase pathways mediated by ERK, JNK, and p38 protein kinases. *Science* 298, 1911–1912.
- Kawamura-Saito, M., Yamazaki, Y., Kaneko, K., Kawaguchi, N., Kanda, H., Mukai, H., Gotoh, T., Motoi, T., Fukayama, M., Aburatani, H., et al. (2006). Fusion between CIC and DUX4 up-regulates PEA3 family genes in Ewing-like sarcomas with t(4 ; 19)(q35 ; q13) translocation. *Hum. Mol. Genet.* 15, 2125–2137.
- Lake, D., Correa, S.A., and Muller, J. (2016). Negative feedback regulation of the ERK1/2 MAPK pathway. *Cell. Mol. Life Sci.* 73, 4397–4413.
- LeBlanc, V.G., Firme, M., Song, J., Chan, S.Y., Lee, M.H., Yip, S., Chittaranjan, S., and Marra, M.A. (2017). Comparative transcriptome analysis of isogenic cell line models and primary cancers links capicua (CIC) loss to activation of the MAPK signalling cascade. *J. Pathol.* 242, 206–220.
- Lim, B., Samper, N., Lu, H., Rushlow, C., Jimenez, G., and Shvartsman, S.Y. (2013). Kinetics of gene depression by ERK signaling. *Proc. Natl. Acad. Sci. U S A* 110, 10330–10335.
- Lin, Y.K., Wu, W., Ponce, R.K., Kim, J.W., and Okimoto, R.A. (2020). Negative MAPK-ERK regulation sustains CIC-DUX4 oncoprotein expression in undifferentiated sarcoma. *Proc. Natl. Acad. Sci. U S A* 117, 20776–20784.
- Okimoto, R.A., Wu, W., Nanjo, S., Olivas, V., Lin, Y.K., Ponce, R.K., Oyama, R., Kondo, T., and Bivona, T.G. (2019). CIC-DUX4 oncoprotein drives sarcoma metastasis and tumorigenesis via distinct regulatory programs. *J. Clin. Invest.* 129, 3401–3406.
- Packer, L.M., East, P., Reis-Filho, J.S., and Marais, R. (2009). Identification of direct transcriptional targets of (V600E)BRAF/MEK signalling in melanoma. *Pigment Cell Melanoma Res.* 22, 785–798.
- Pearson, G., Robinson, F., Beers Gibson, T., Xu, B.E., Karandikar, M., Berman, K., and Cobb, M.H. (2001). Mitogen-activated protein (MAP) kinase pathways: regulation and physiological functions. *Endocr. Rev.* 22, 153–183.
- Pratilas, C.A., Taylor, B.S., Ye, Q., Viale, A., Sander, C., Solit, D.B., and Rosen, N. (2009). (V600E)BRAF is associated with disabled feedback inhibition of RAF-MEK signaling and elevated transcriptional output of the pathway. *Proc. Natl. Acad. Sci. U S A* 106, 4519–4524.
- Roch, F., Jimenez, G., and Casanova, J. (2002). EGFR signalling inhibits Capicua-dependent repression during specification of *Drosophila* wing veins. *Development* 129, 993–1002.
- Tseng, A.S., Tapon, N., Kanda, H., Cigizoglu, S., Edelmann, L., Pellock, B., White, K., and Hariharan, I.K. (2007). Capicua regulates cell proliferation downstream of the receptor tyrosine kinase/ras signaling pathway. *Curr. Biol.* 17, 728–733.
- Wang, B., Krall, E.B., Aguirre, A.J., Kim, M., Widlund, H.R., Doshi, M.B., Scicska, E., Sulahian, R., Goodale, A., Cowley, G.S., et al. (2017). ATXN1L, CIC, and ETS transcription factors modulate sensitivity to MAPK pathway inhibition. *Cell Rep.* 18, 1543–1557.
- Weissmann, S., Cloos, P.A., Sidoli, S., Jensen, O.N., Pollard, S., and Helin, K. (2018). The tumor suppressor CIC directly regulates MAPK pathway genes via histone deacetylation. *Cancer Res.* 78, 4114–4125.
- Yoshimoto, T., Tanaka, M., Homme, M., Yamazaki, Y., Takazawa, Y., Antonescu, C.R., and Nakamura, T. (2017). CIC-DUX4 induces small round cell sarcomas distinct from Ewing sarcoma. *Cancer Res.* 77, 2927–2937.
- Zeliadt, N.A., Mauro, L.J., and Wattenberg, E.V. (2008). Reciprocal regulation of extracellular signal regulated kinase 1/2 and mitogen activated protein kinase phosphatase-3. *Toxicol. Appl. Pharmacol.* 232, 408–417.
- Zhang, Z., Kobayashi, S., Borczuk, A.C., Leidner, R.S., Laframboise, T., Levine, A.D., and Halmos, B. (2010). Dual specificity phosphatase 6 (DUSP6) is an ETS-regulated negative feedback mediator of oncogenic ERK signaling in lung cancer cells. *Carcinogenesis* 31, 577–586.

iScience, Volume 23

## **Supplemental Information**

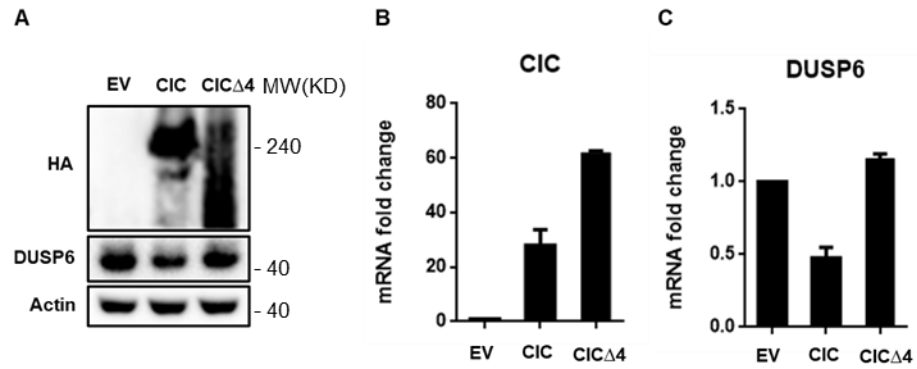
### **CIC Is a Mediator of the ERK1/2-DUSP6**

#### **Negative Feedback Loop**

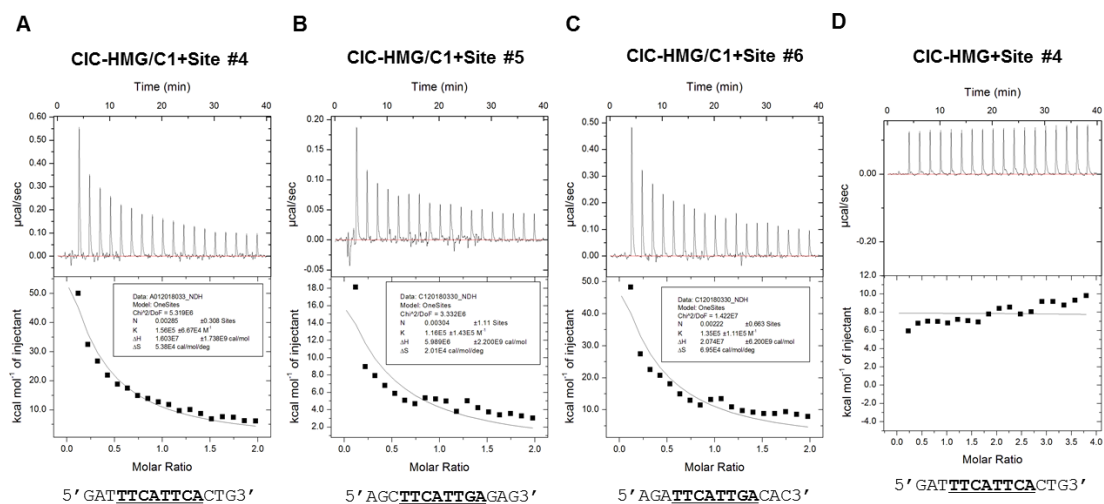
**Yibo Ren, Zhenlin Ouyang, Zhanwu Hou, Yuwei Yan, Zhe Zhi, Mengjin Shi, Mengtao Du, Huadong Liu, Yurong Wen, and Yongping Shao**

## Supplemental Information

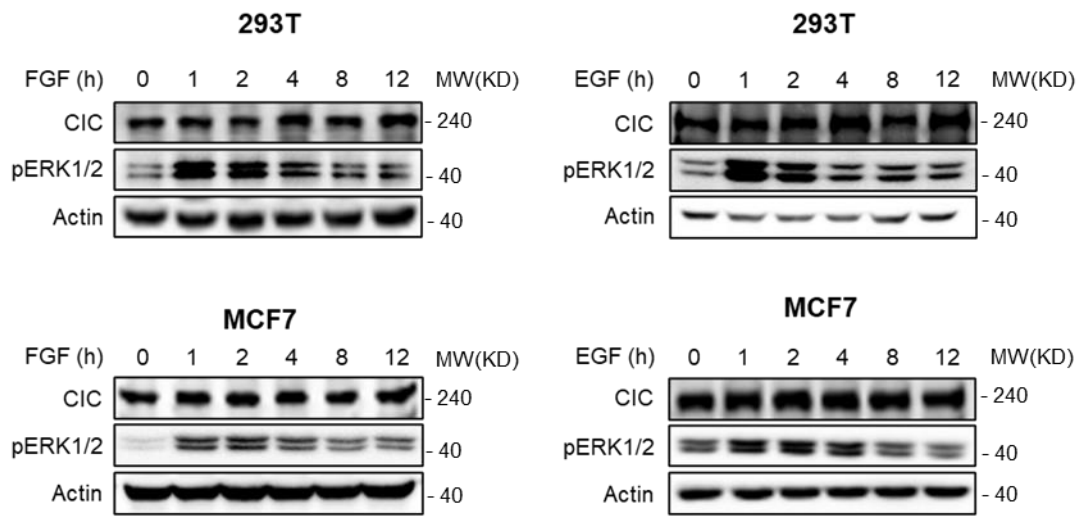
### Supplemental Figures



**Figure S1. CICΔ4 mutation causes protein degradation and loss of repressor activity toward DUSP6 (Related to Figure 1).** (A) 293T<sup>CIC</sup> cells were transfected with empty vector (EV), HA-CIC, HA-CICΔ4 plasmids for 48 hours and lysed for western blot analysis. (B-C) Cells were treated as in (A) and total RNAs were isolated for qRT-PCR analysis on CIC and DUSP6.

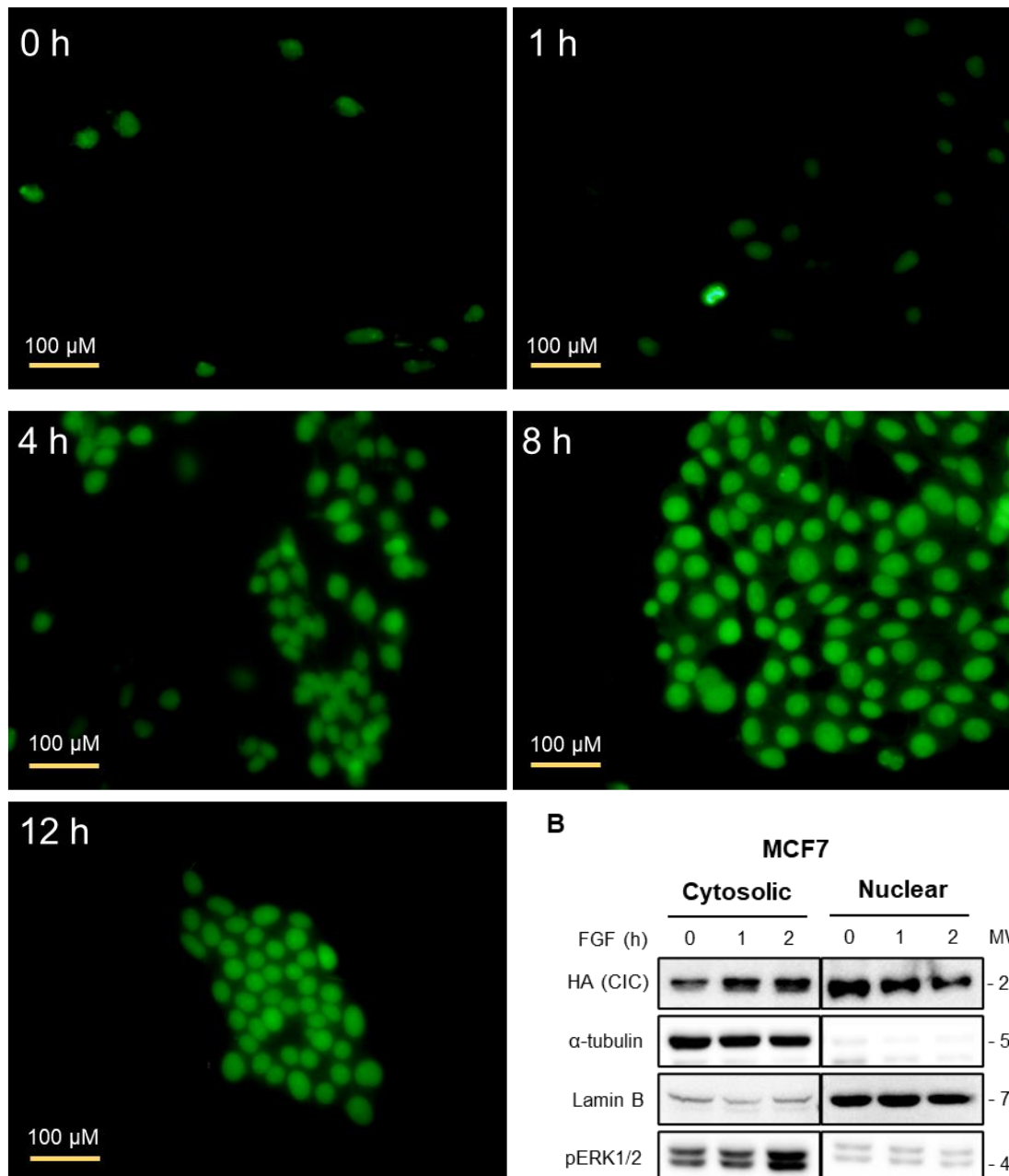


**Figure S2. Binding of CIC-HMG/C1 to cis elements in DUSP6 promoter (Related to Figure 3).** (A-C) ITC analysis CIC-HMG/C1 binding to DNA fragments containing site #5 (A), #6 (B) and #6 (C) in DUSP6 promoter. (D) ITC analysis of CIC-HMG binding to site #4.



**Figure S3. FGF/EGF stimulation does not alter CIC expression in 293T and MCF7 cells within 12 hours (Related to Figure 4).** MCF7 or 293T cells were treated with FGF (10 ng/mL) or EGF (75 ng/mL) for different time points and lysed for western blot analysis.

A

293T<sup>CIC</sup>/HA-CIC

**Figure S4. FGF promotes nuclear export of CIC (Related to Figure 4).** (A) 293T<sup>CIC</sup> cells transduced with WT HA-CIC lentivirus were treated with 10 ng/mL FGF for various time and immunofluorescence staining were performed to examine the subcellular distribution of HA-CIC using HA-tag antibody. (B) MCF7 cells were transfected with HA-CIC expressing plasmid for 48 hours. Cells were treated with 10 ng/mL FGF for 0, 1, 2 hours and subjected to nuclear/cytoplasmic fractionation. Nuclear and cytoplasmic lysates were comparatively analyzed by western blot.

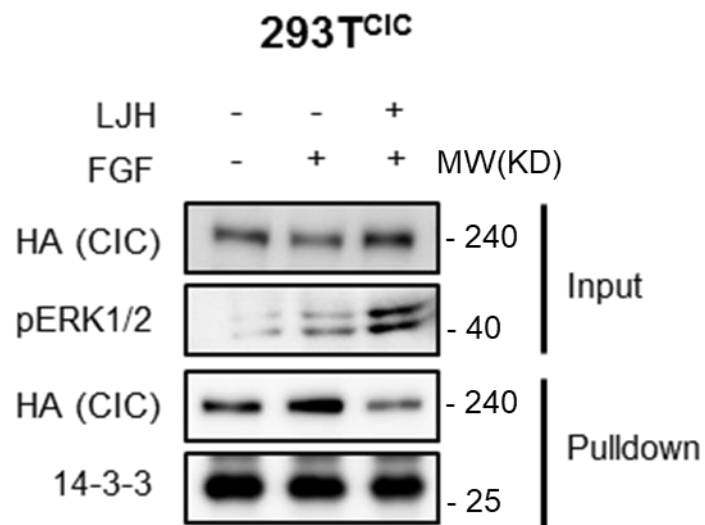


**Figure S5. 14-3-3 interacts with CIC *in vivo* (Related to Figure 6).** Protein pull-down assay performed using purified recombinant 14-3-3 and lysates of 293T<sup>CIC</sup> cells that are transfected with HA-CIC and treated with -/+FGF, -/+LJH658.

## Supplemental Tables

**Table S1. X-ray data collection and refinement statistics. Statistics for the highest resolution shell are shown in parentheses. (Related to Figure 6)**

Crystal	14-3-3 in complex with CIC173pS	14-3-3 in complex with CIC301pS
<b>Data collection</b>		
Spacegroup	P2 <sub>1</sub> 2 <sub>1</sub> 2 <sub>1</sub>	P2 <sub>1</sub> 2 <sub>1</sub> 2 <sub>1</sub>
a, b, c (Å)	70.2, 80.8, 107.1	69.7, 79.5, 106.3
$\alpha$ , $\beta$ , $\gamma$ (°)	90, 90, 90	90, 90, 90
Resolution (Å)	33.34-2.65 (2.74-2.65)	44.17-2.00 (2.07-2.00)
<i>R</i> <sub>merge</sub>	0.147 (1.27)	0.113 (1.38)
<i>R</i> <sub>meas</sub>	0.154 (1.37)	0.117 (1.48)
Multiplicity	12.8 (12.0)	12.8 (12.4)
CC(1/2)	0.998 (0.64)	1 (0.61)
CC*	1 (0.80)	1 (0.82)
<i>I</i> / $\sigma$ ( <i>I</i> )	11.1 (1.0)	16.9 (1.1)
Completeness (%)	99.75 (99.17)	99.81 (99.00)
Wilson B-factor (Å <sup>2</sup> )	72.74	41.16
<b>Refinement</b>		
Total Reflections	234546 (21565)	522995 (48786)
Unique Reflections	18361 (1800)	40758 (3950)
<i>R</i> <sub>work</sub>	0.2154	0.1909
<i>R</i> <sub>free</sub>	0.2721	0.2306
Number of atoms:		
Macromolecules	3740	3808
Water	0	165
Average B-factor (Å <sup>2</sup> )	81.37	52.52
Protein (Å <sup>2</sup> )	81.37	52.37
Water (Å <sup>2</sup> )	0	55.92
Ramachandran plot:		
Favored/Allowed (%)	96.7/3.2	98.5/1.5
Root-Mean-Square-Deviation:		
Bond lengths (Å)	0.005	0.008
Bond Angle (°)	0.72	0.85
PDB code	6KZH	6KZG

## **Transparent Methods**

### **Reagent**

AZD6244, LJH685, SCH772984 were purchased from Selleck Chemicals LLC (Houston, TX, USA). Human FGF was purchased from PeproTech (Rocky Hill, NJ, USA).

### **Cell culture**

Human 293T cell and MCF7 cell were purchased from ATCC (Manassas, VA, USA). 1205Lu cells were gifted by Dr. Meenhard Herlyn at The Wistar Institute. 293T and MCF7 cells were cultured in high-glucose DMEM with 10% fetal bovine serum (FBS) and penicillin-streptomycin (200 µg/mL). 1205Lu cells were cultured in RPMI-1640 medium with 10% FBS and penicillin/streptomycin.

### **siRNA transfection**

Cells were transfected with 12.5 nM small-interfering RNA and Lipofectamine RNAiMAX (Thermo Fisher Scientific, Rockford, IL, USA) for 72 h. Non-targeting siRNA control (5'-UUCUCCGAACGUGUCACGU-3') and siRNAs for CIC (#1: 5'-CCGUAUGCAGCACAAGAAA-3'; #2: 5'-GUAUGCAGCACAAGAAAGA-3') were purchased from Shanghai GenePharma Co., Ltd. (Shanghai, China).

### **CRISPR-Cas9-mediated CIC knockout in 293T and MCF7 cells**

The CIC targeting sgDNA (5'-AGGAAACGGGACTCATCTTCT-3') was cloned into the LentiCRSPRV2 vector and the resulting plasmid was transfected into MCF7 or 293T cells using XtremeGENE™ HP DNA Transfection Reagent (Roche, Basel, Switzerland). After 24h, Cells were puromycin selected for 48 hours and then serial-diluted in a 96 well plate for clone formation. Genomic DNAs were isolated for each individual clones and CIC knockout was verified by PCR amplifying the sgRNA-targeted genomic region, followed by TA cloning and DNA sequencing.

### **Western blotting**

Western blotting was performed as previously described (Han et al., 2018). Antibody against DUSP6 (clone EPR129Y, ab76310) was from Abcam (Cambridge, UK). Antibody against HA-tag (clone 6E2, #2367), Phospho-p44/42MAPK (Thr202/Tyr204, clone197G2, #4377), Myc-tag (clone 71D10, #2278) were from Cell Signaling Technology (Beverly, MA, USA). Anti- $\beta$ -actin (#A2066) was from Sigma (Ronkonkoma, NY, USA). Anti- $\alpha$ -Tubulin (#961216), anti-Lamin B1 (Clone #919007) were from R&D Systems (Minneapolis, MN, USA). CIC antibodies were purchased from Bethyl Laboratories (A301-204A) (Montgomery, Texas, USA) and Abcam (ab123822)( Cambridge, MA, USA).

### **Quantitative RT-PCR**

Total RNA was isolated using TRIzol reagent (Thermo Fisher Scientific) and reverse transcribed into cDNA using iScript cDNA Synthesis Kit (Bio-Rad, Hercules, California, USA). Quantitative PCR was performed in a CFX Connect Real-Time PCR Detection System (Bio-Rad) using iQ SYBR Supermix Kit (Bio-Rad). Relative mRNA levels were calculated using the  $\Delta$ Ct method. Each Quantitation of mRNA levels represents data from three independent experiments. The following primer sets were used: CIC (Forward, 5'-GGTACTGGCAAGAAGGTGAAGG-3', Reverse, 5'-ACTCAGGCAACTCAGCAAAGC-3'); DUSP6 (Forward, 5'-TGTCCCAGTTTTCCCTGAG-3', Reverse, 5'-CAGTGACTGAGCGGCTAATG-3'); ETV5 (Forward, 5'-TCAGCAAGTCCCTTTTATGGTC-3', Reverse, 5'-GCTCTTCAGAATCGTGAGCCA-3'); Actin (Forward, 5'-TACCTCATGAAGATCCTCACC-3', Reverse, 5'-TTTCGTGGATGCCACAGGAC-3').

### **Dual-luciferase reporter assay**

Cells were co-transfected with pGL3-DUSP6 promoter reporter construct, pRL-TK and other indicated plasmids in 12-well plates using X-tremeGENE HP DNA transfection reagent. Cells were harvested after 48 hours for dual luciferase assay using a Dual-Luciferase® Reporter Assay Kit (Promega, Madison, WI, USA) according to manufacturer's instruction. Luminescence was detected by a FlexStations 3 microplate reader (Molecular Devices, Sunnyvale, CA, USA).

### **Protein overexpression and purification**

The CIC-HMG/C1 fusion protein contains an N-terminal His tag followed by HMG domain (a.a. 188-288) and C1 domain (a.a. 1401-1609) in turn. The CIC-HMG protein contains the HMG domain only with N-terminal His tag. For CIC-HMG/C1 or CIC-HMG recombinant protein purification, *E.coli* BL21 (DE3) cells transformed with pET28a-CIC-HMG/C1 or pET28a-CIC-HMG plasmid were grown to an OD<sub>600</sub> of 0.6 in LB medium supplemented with 100 µg/ml Kanamycin at 37 °C. The cells were then induced with 1 mM IPTG at 28 °C for 8 hours and harvested by centrifugation at 7000 g, 4 °C. The cell pellets were resuspended in lysis buffer (50 mM HEPES, pH 7.5) and lysed by sonication at 4 °C. The lysate was further centrifuged at 25000 g to remove cell debris. Filtered lysate supernatant was loaded onto a HiTrap™ Sepharose™ HP Ion Exchange Column (GE healthcare, Chicago, Illinois, USA) pre-equilibrated with loading buffer (50 mM HEPES, pH 7.5). Column bound proteins were then eluted with elution buffer (50 mM HEPES, pH 7.5) containing a gradient of 0.05M-1M NaCl using an AKTA purifier system. The fractions containing the eluted proteins were concentrated and loaded on Superdex75 16/60 (GE Healthcare) size exclusion chromatography column in 20 mM Tris pH 7.5, 150mM NaCl, 10% glycerol. The main protein fractions were concentrated. The protein concentration was measured with a NanoDrop ® spectrometer (Thermo Fisher Scientific) using the extinction coefficient generated from Ex-PASy

ProtParam program. The recombinant 14-3-3 $\theta$  protein contains an N-terminal His tag and 14-3-3 amino acids 1-234. For 14-3-3 $\theta$  purification, *E. coli* BL21 cells harboring pET28a-14-3-3 $\theta$  plasmid were grown to OD<sub>600</sub>=0.6 and induced with 1 mM IPTG for 8 h. Cells were lysed as above and His-tagged 14-3-3 $\theta$  protein was purified using affinity chromatography (HisTrap™ HP Column, GE Healthcare) followed by size exclusion chromatography (Superdex75 16/60 column, GE Healthcare).

### **Isothermal titration calorimetry (ITC)**

The ITC experiments were performed in a Microcal ITC200 calorimeter (GE Healthcare) at room temperature. For CIC/DNA titration experiment, complementary single-stranded oligonucleotides (20 bp) containing putative CIC binding sites were annealed to form double-stranded DNAs and purified using size exclusion chromatography. Purified DNAs were buffer exchanged to 20mM Tris pH 7.5, 150 mM NaCl, 10% glycerol. The titrations were carried by injecting CIC-HMG/C1 recombinant protein (70-100  $\mu$ M) into DNA solutions (7-10  $\mu$ M). The injection started with a 0.4  $\mu$ L one followed by 19 successive injections of 2  $\mu$ L each with an injection interval of 120s. Data were analyzed using the Microcal Origin program. The following oligonucleotides were used in this experiment: Site #4 (Forward, 5'-TTGGATTCATTCACTGGGG-3'; Reverse, 5'-CCCCAGTGAATGAAATCCAA-3'), Site #5 (Forward, 5'-GGCAGCTTCATTGAGAGAGA-3'; Reverse, 5'-TCTCTCTCAATGAAGCTGCC-3') , Site #6 (Forward, 5'-GAGAGATTCATTGACACTAA-3'; Reverse, 5'-TTAGTGTCATGAATCTCTC-3'). For CIC/14-3-3 $\theta$  interaction experiment, titration was carried out by injecting 120-200  $\mu$ M CIC peptides into 12-20  $\mu$ M 14-3-3 $\theta$  solution following the same protocol described above. The following CIC peptides were used: RTQpSLSAL, RTQSLSAL, RSMpSETGT, RSMSETGT.

### **Electrophoretic mobility shift assay (EMSA)**

The EMSA experiments were performed according to the manufacturer's instruction of the LightShift Chemiluminescent EMSA Kit (Thermo Fisher Scientific). The oligonucleotides used for EMSA had the same sequence as those in the ITC experiment except that the 5' end of the forward oligonucleotide is biotin labeled. Oligonucleotides were annealed and double-stranded DNA fragments were purified using size exclusion chromatography. The binding reactions were carried out in 20  $\mu$ L of 1x binding buffer (10 mM Tris, 50 mM KCl, 1 mM DTT, pH 7.5, 2.5% glycerol, 5 mM MgCl<sub>2</sub>, 50 ng/ $\mu$ L Poly (dI•dC), 0.05% NP40) containing 1 pmol purified DNA and a titration of recombinant CIC-HMG/C1 for 30 min. The reaction mixtures were loaded onto a 5% native polyacrylamide gel and separated in 0.5  $\times$  TBE at 100 V on ice. Reaction mixtures were then transferred to Biorad B nylon membranes (Thermo Fisher Scientific) and cross-linked to the membrane in a CL-1000 UV cross-linker (UVP) for 5 min. Reaction products were detected using streptavidin-horseradish peroxidase (HRP). The oligonucleotide sequences for mutant Site #4 are: Forward, 5'-TTGGATTTAGCTCACTGGGG-3'; Reverse, 5'-CCCCAGTGAGCTAAATCCAA-3'

### **Chromatin Immunoprecipitation (ChIP) Assay**

Cells grown to 80-90% confluency were fixed with 1 % formaldehyde for 10 minutes at room temperature and then stopped with 0.125M glycine. After PBS washing, cells were scraped and collected by centrifugation. Cells were then lysed in cell lysis buffer (20 mM Tris-HCL, pH 8.0, 85 mM KCL, 0.5% NP40, and protease inhibitor cocktail (Roche)) and centrifuged to collect the nucleus. Nucleus pellet was resuspended in SDS lysis buffer (1% SDS, 10 mM EDTA, 50 mM Tris-HCL, pH 8.1 and protease inhibitor cocktail) and sonicated to shear the DNA. Chromatin immunoprecipitation was performed overnight at 4  $^{\circ}$ C using diluted sonicated lysates (1:5 in

dilution buffer, 0.01% SDS, 1.1% Triton X-100, 1.2 mM EDTA, 16.7 mM Tris-HCL, pH 8.1, 167 mM NaCl plus protease inhibitors) and IgG or CIC antibody. Antibody-Chromatin complexes were captured by the protein A/G Plus-Agarose beads (Santa Cruz, CA, USA) and washed in low salt wash buffer (0.1% SDS, 1% Triton X-100, 2 mM EDTA, 20 mM Tris-HCL, pH 8.1, 500 mM NaCl), high salt wash buffer (0.1% SDS, 1% Triton X-100, 2 mM EDTA, 20 mM Tris-HCL, pH 8.1, 500 mM NaCl), LiCl wash buffer (0.25 M LiCl, 1% NP40, 1% deoxycholate, 1 mM EDTA, 10 mM Tris-HCL, pH 8.1) and TE Buffer (10 mM Tris-HCL, 1 mM EDTA, pH 8.0). Protein/DNA complexes were eluted with elution buffer (1% SDS, 0.1 M NaHCO<sub>3</sub>) and decrosslinked in 0.2 M NaCl at 65 °C overnight. DNA was then purified by PCR cleanup columns. Immunoprecipitated chromatin DNA was detected by qPCR using iQ SYBR Green Supermix (Bio-Rad). The following primers were used for PCR. NC\_forward, 5'-ATGGTTGCCACTGGGGATCT-3'; NC\_reverse, 5'-TGCCAAAGCCTAGGGGAAGA-3'; DUSP6\_forward, 5'-CCTCCCCTCTCAGTAGCACG-3'; DUSP6\_reverse, 5'-ACAGAAGTAAAGCCGGAGGT-3'

### **Immunofluorescence**

293T<sup>CIC</sup> cells transduced with WT HA-CIC lentivirus were plated on coverslips in 24-well plates. After overnight culturing, cells were treated with 10 ng/mL FGF for various time (0, 1, 4, 8, 12 hours) and washed twice with cold PBS. Cells were then fixed in 3.7% formaldehyde for 15 min, and permeabilized in 0.1% Triton X-100 for 2 min. After PBS washing and 2% BSA blocking, cells were incubated with anti-HA antibody at 4 °C overnight. The next day, cells were washed and stained with FITC-conjugated secondary antibody. Staining was visualized by an inverted fluorescence microscope system (Olympus, Tokyo, Japan).

### **Nuclear and Cytoplasmic Protein Extraction**

Nuclear/Cytoplasmic fractionation was then performed using the Nuclear and Cytoplasmic Protein Extraction kit (Tiangen Biotech, Beijing, China) according to manufacturer's instruction.

### ***In Vivo* detection of CIC phosphorylation**

293T<sup>CIC</sup> cells were transfected with HA-CIC expressing plasmid for 48 hours and treated with -/+ 10 ng/mL FGF for 4 hours. Cells were washed in PBS and lysed in lysis buffer (20 mM Tris-HCl, pH7.5, 150 mM NaCl, 1 mM EDTA, 1% NP40, 0.1% SDS, 1% sodium deoxycholate) supplemented with protease and phosphatase inhibitor cocktails (Roche, Basel, Switzerland). HA-CIC was immunoprecipitated from the lysate using anti-HA Magnetic Beads (Thermo Fisher Scientific) and eluted with 50 mM NH<sub>4</sub>HCO<sub>3</sub>. Anti-HA immunoprecipitates were collected and digested in 50 mM NH<sub>4</sub>HCO<sub>3</sub> with sequencing grade trypsin. Phosphopeptides were then enriched using Pierce™ TiO<sub>2</sub> Phosphopeptide Enrichment and Clean-up Kit (Thermo Fisher Scientific) according to the manufacturer's instruction. The purified phosphopeptides were subsequently injected onto an AB SCIEX QTRAP 6500+ using Eksigent nanoflex cHiPLC system with a reverse-phase ChromXP C18-CL column for peptides separation at the flow rate of 300 nLmin<sup>-1</sup>. Peptides were eluted using a 62 min gradient from 95% solvent A (H<sub>2</sub>O, 0.1% formic acid) and 5% B (acetonitrile, 0.1% formic acid) to 50% B in 41 min, 6 min at 90%B, and back to 5% for 10 min. The instrument was set to monitor 50 to 100 transitions in each sample with a dwelling time of 100 ms per transition. Eluted peptides were then electrosprayed into the mass spectrometer and MS/MS spectra were collected in the linear ion trap mode with a mass range of 100-120039. The total ion chromatograms for the peptides eluted at identical time provided measurement of their relative quantities using Skyline software.

### ***In Vitro* kinase Assay**

Wild type CIC-HMG domain (aa 156-330) which contains putative p90RSK phosphorylation sites as well as mutant variants (S173A, S301A and S173A/S301A) were expressed in *E.coli* BL21 and purified using affinity and size exclusion chromatography as described above. For *in vitro* kinase assay, 1 or 3  $\mu\text{M}$  of protein substrates (CIC-HMG) were incubated with 10 ng/mL of activated GST-p90RSK (R&D Systems) and 0.5 mM ATP in 1 $\times$  NEBuffer (NEB) at 30  $^{\circ}\text{C}$  for 45 min. The reaction products were analyzed by the ADP-Glo<sup>TM</sup> Kinase Assay Kit (Promega) following the manufacturer's instruction.

### **Protein pull-down assay**

293T<sup>CIC</sup> cells were transfected with WT or S173A/S301A HA-CIC expressing plasmids for 24 hours and treated with or without 10 ng/mL FGF and/or 10  $\mu\text{M}$  LJH685 for 3 hours. Cells were then lysed in cell lysis buffer (50mM Tris-HCL, pH 7.5, 150 mM NaCl, 1% NP40, 1mM EDTA, and protease inhibitor cocktail tablet) and centrifuged to collect the cell lysates. Purified His-14-3-3 $\theta$  protein was incubated with cell lysates (containing HA-CIC) at 4 $^{\circ}\text{C}$  for 4 hours. CIC/14-3-3 $\theta$  protein complexes were precipitated using Ni-NTA Magnetic Beads (NEB). Protein/bead complexes were washed 3 times with washing buffer (50 mM Tris-HCl, pH7.5, 150mM NaCl, 1% NP40, 1mM EDTA), eluted with SDS sample buffer and analyzed by western blotting.

### **Crystallization and data collection**

The complexes of 14-3-3 $\theta$  protein and CIC phospho-peptides were mixed at a molar ratio of 1:2 protein/peptide and a final concentration of 15 mg/ml in 20 mM Tris, 150 mM NaCl, 5% Glycerol, 2 mM MgCl<sub>2</sub> pH 8.0 for 1 h on ice and then set-up in a 392-well Hampton crystallization plate using the sitting-drop method by mixing 0.5  $\mu\text{l}$  protein solution and 0.5  $\mu\text{l}$  reservoir solution at 20 $^{\circ}\text{C}$  for sparse matrix screens (Molecular Dimensions and Hampton Research). The 14-3-3 $\theta$  and

peptide1 (RTQpSLSAL) complex was crystallized in 0.2 M Sodium chloride, 0.1 M HEPES pH 7.5, 25% w/v Polyethylene glycol 3,350, and the 14-3-3 $\theta$  and peptide2 (RSMpSETGT) complex was crystallized in 8% v/v Tacsimate<sup>TM</sup> pH 6.0, 20% w/v Polyethylene glycol 3,350. All the obtained crystals were soaked in cryoprotectant solution containing the reservoir solution supplemented with 15–30% (v/v) glycerol and mounted in loops and cryo-cooled before data collection. X-ray diffraction data were collected at the Beam-lines BL18U1 at Shanghai Synchrotron Radiation Facility (SSRF) at 100 K. the data were processed and scaled with HKL3000 and the XDS suite (Kabsch et al., 2010). Data collection details and statistics are supplemented in Table S1.

### **Structure determination and refinement**

Structures were solved by molecular replacement implemented in the Phaser program suite (McCoy et al., 2007), using the structure of the *Homo sapiens* 14-3-3 $\theta$  protein tau isoform (PDB: 5IQP) as search model (Xiao et al., 1995). The program COOT and PHENIX suite were used for further manual model rebuilding and refinement (Emsley et al., 2004, Adams et al., 2010). The 14-3-3 $\theta$  in complex with pS301 peptide and pS173 peptide were solved in 2.0 Å and 2.65 Å respectively, both in P212121 space group with similar cell parameter of a=70 Å, b=80 Å and c=106 Å. The final structure models were refined with  $R_{\text{work}}/R_{\text{free}}$  of 0.1909/0.2306 for 14-3-3 $\theta$  in complex with pS301 peptide and 0.2154/0.2721 for 14-3-3 $\theta$  in complex with pS173. All the 8 residues (298-305) were observed in the pS301 complex, while in the pS173 complex only central 5 residues (171-175) were traceable. All the structures exhibit good Ramachandran plot and favorable stereochemistry, and detailed refinement statistics are summarized in Table S1. Figures were created using PyMOL (<http://www.pymol.org>).

## Supplemental Reference

Adams, P.D., Afonine, P.V., Bunkoczi, G., Chen, V.B., Davis, I.W., Echols, N., Headd, J.J., Hung, L.W., Kapral, G.J., Grosse-Kunstleve, R.W. et al. (2010) PHENIX: a comprehensive Python-based system for macromolecular structure solution. *Acta Crystallogr D Biol Crystallogr* *66*, 213-221.

Emsley, P. and Cowtan, K. (2004) Coot: model-building tools for molecular graphics. *Acta Crystallogr D Biol Crystallogr* *60*, 2126-2132.

Han, S., Ren, Y., He, W., Liu, H., Zhi, Z., Zhu, X., Yang, T., Rong, Y., Ma, B., Purwin, T.J. et al. (2018) ERK-mediated phosphorylation regulates SOX10 sumoylation and targets expression in mutant BRAF melanoma. *Nat Commun* *9*, 28.

Kabsch, W. (2010) Xds. *Acta Crystallogr D Biol Crystallogr* *66*, 125-132.

McCoy, A.J. (2007) Solving structures of protein complexes by molecular replacement with Phaser. *Acta Crystallogr D Biol Crystallogr* *63*, 32-41.

Xiao, B., Smerdon, S.J., Jones, D.H., Dodson, G.G., Soneji, Y., Aitken, A. and Gamblin, S.J. (1995) Structure of a 14-3-3 protein and implications for coordination of multiple signalling pathways. *Nature* *376*, 188-191.